Structural Analysis
Part III - X-ray tools

Session 2:

X-ray scattering and diffraction

Discovery of X-rays triggered many technological and scientific developments

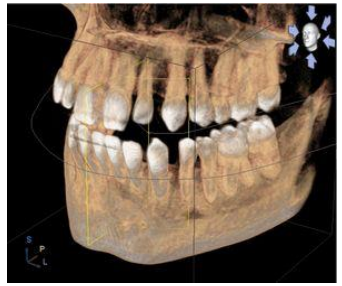

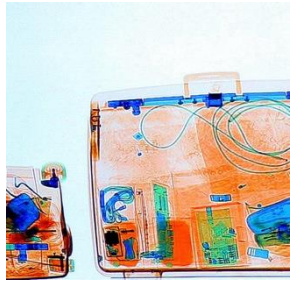

Table 1.1 Nobel Prizes awarded in the field of x-ray research.

Year	Recipient(s)	Research discipline
1901	W. C. Röntgen	Physics; discovery of x-rays
1914	M. von Laue	Physics; x-ray diffraction from crystals
1915	W. H. Bragg and W. L. Bragg	Physics; crystal structure derived from x-ray diffraction
1917	C. G. Barkla	Physics; characteristic radiation of elements
1924	K. M. G. Siegbahn	Physics; x-ray spectroscopy
1927	A. H. Compton	Physics; scattering of x-rays by electrons
1936	P. Debye	Chemistry; diffraction of x-rays and electrons in gases
1946	H. J. Muller	Medicine; discovery of x-ray-induced mutations
1962	M. Perutz and J. Kendrew	Chemistry; structures of myoglobin and haemoglobin
1962	J. Watson, M. Wilkins, and F. Crick	Medicine; structure of DNA
1964	D. Crowfoot-Hodgkin	Chemistry; structure of penicillin
1976		
1979		
1981		
1985		
1988		
1997		
2003		
2006		
2009		
2012		
2018		

[1]Work using synchr

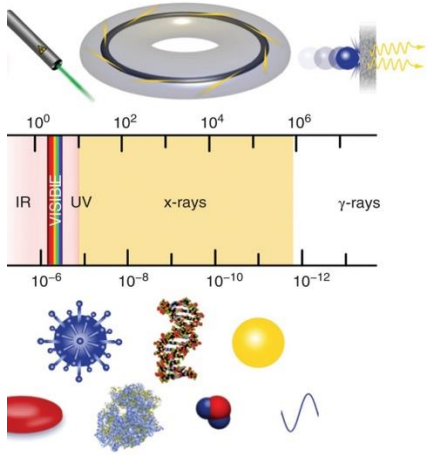

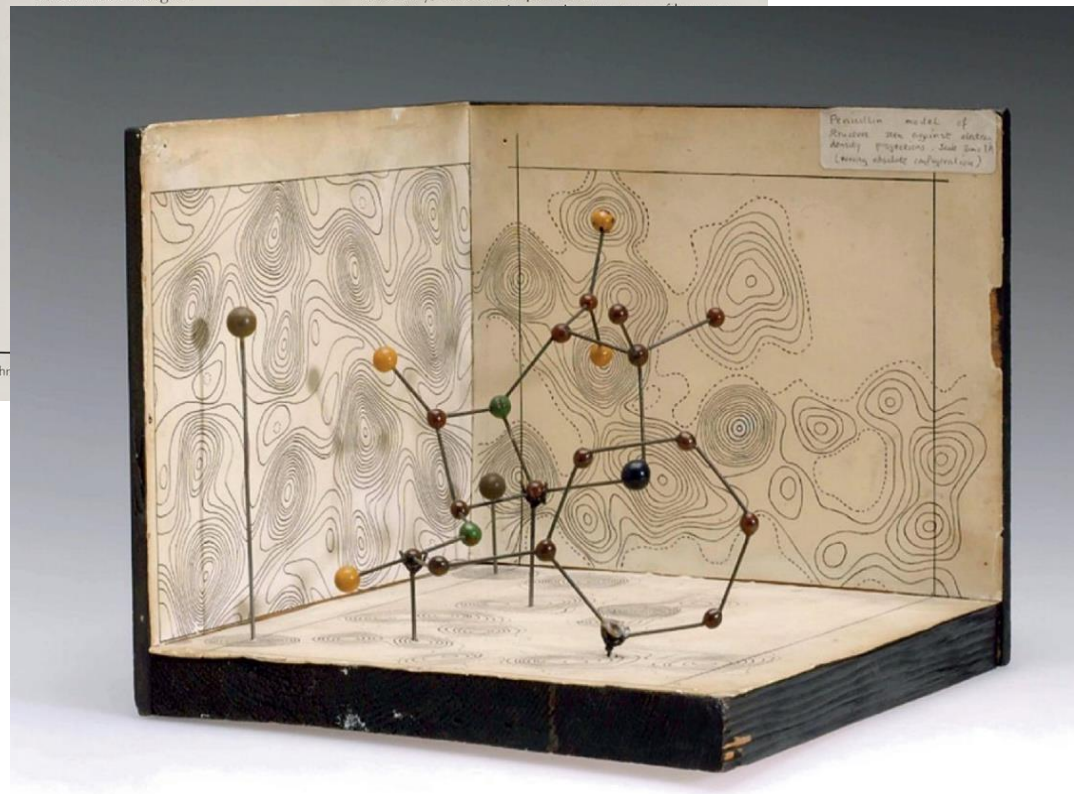

⇓

λ matched to molecular structures

⇓

⇒ diffraction exps.

Why care about x-ray diffraction of crystals?

Why should we care about x-rays, crystals, lattices, etc?

Source:
The Cambridge Structural Database (CSD)

Organic
43%

Metal-Organic
57%
At least one transition metal, lanthanide, actinide or any of Al, Ga, In, Tl, Ge, Sn, Pb, Sb, Bi, Po

Not Polymeric
89%

Polymeric: 11%

Single Component
56%

Multi Component
44%

Organic
- Drugs
- Agrochemicals
- Pigments
- Explosives
- Protein ligands

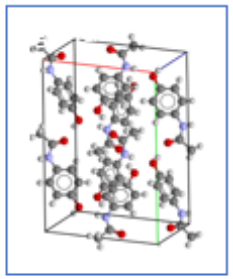

Metal-Organic
- Metal Organic Frameworks
- Models for new catalysts
- Porous frameworks for gas storage
- Fundamental chemical bonding

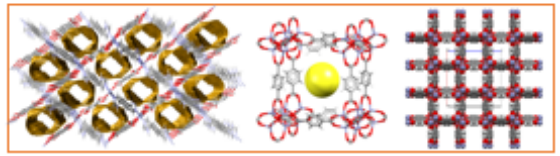

Additional data
- >10,000 polymorph families
- >160,000 melting points
- >700,000 crystal colours
- >600,000 crystal shapes
- >23,000 bioactivity details
- >9,000 natural source data
- > 250,000 oxidation states

Links and subsets
- Drugbank
- Druglike
- MOFs
- PDB ligands
- PubChem
- ChemSpider

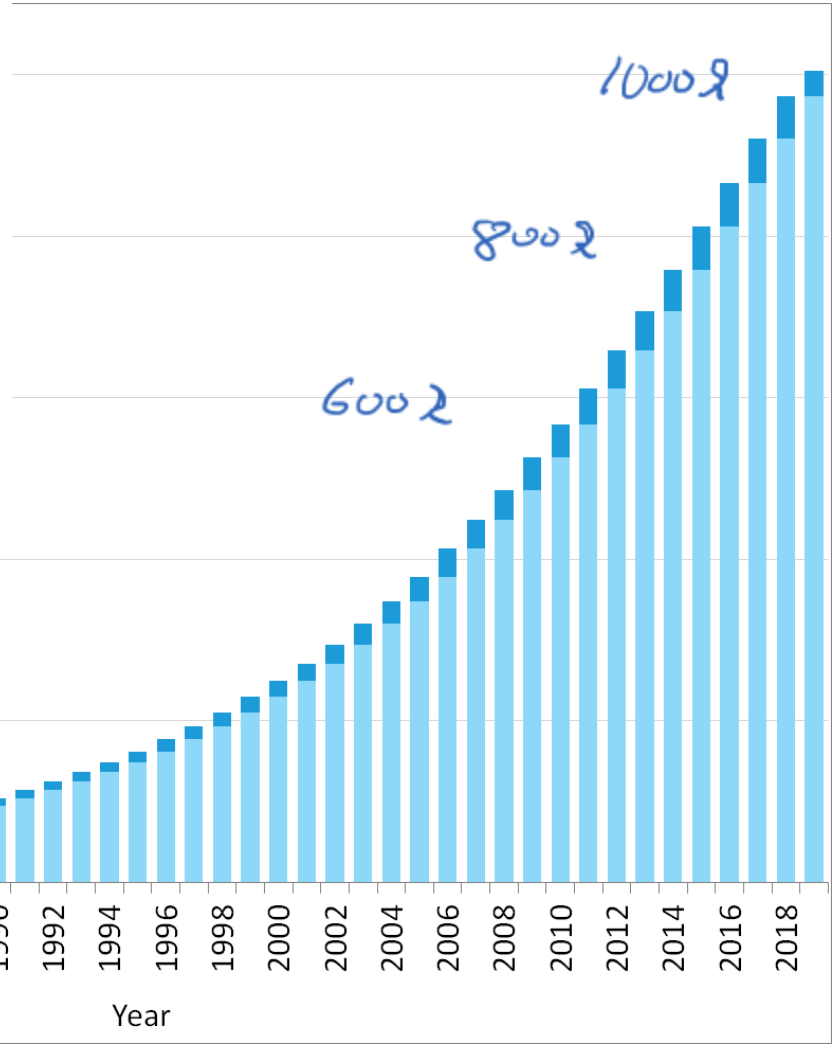

⇒ X-ray diffraction one of most important tools for structural analysis

⇒ Combine with NMR, MS

⇒ X-rays provide electron densities → molecular backbone

https://www.ccdc.cam.ac.uk/solutions/csd-system/components/csd/

Example: Diamondoids – Diamond Molecules

3D structure ⟩ molecules cut out of the diamond lattice

REPORT

Isolation and Structure of Higher Diamondoids, Nanometer-Sized Diamond Molecules

J. E. Dahl, S. G. Liu, R. M. K. Carlson*
+ See all authors and affiliations

Science 03 Jan 2003:
Vol. 299, Issue 5603, pp. 96-99
DOI: 10.1126/science.1078239

Example: Diamondoid molecules

Question: How to figure out that this is not just another organic Compound

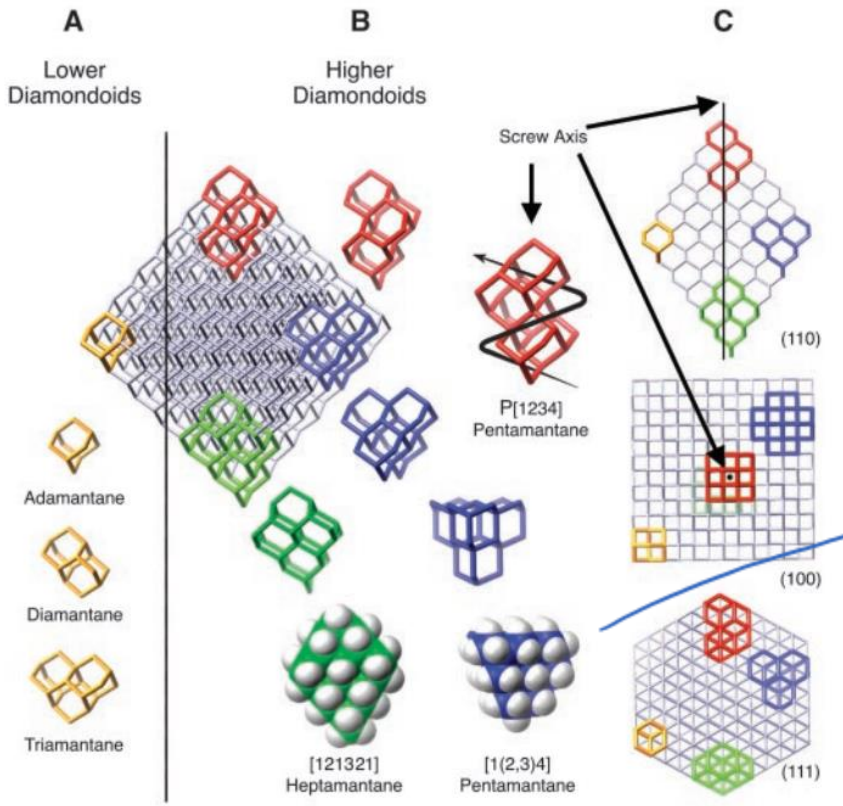

$C_{26}H_{32}$

Fig. 1. The relation between the face-centered cubic diamond lattice and diamondoid structures. (**A**) Adamantane (yellow) is shown superimposed upon the lattice of a 455-carbon octaghedral diamond (some carbons removed for clarity). Adamantane, diamantane, and triamantane (all in yellow) are also shown separate from the diamond lattice. (**B**) Screw-shaped higher diamondoid P [1234] pentamantane (red), pyramidal [1(2,3)4] pentamantane (blue), and rhombus-shaped [121321] heptamantane (green) superimposed upon the diamond lattice and also separate from the lattice. (**C**) The 455-carbon diamond with superimposed diamondoid structures viewed along the (110), (100), and (111) lattice planes showing the diamond lattice faces of the pentamantanes and heptamantane. Views of the P [1234] pentamantane screw axis are indicated by straight arrows. The clockwise helical arrow indicates the groove in the red P [1234] pentamantane molecule.

Supplemental Material: Crystallization for XRD

Crystallization

We crystallized specific higher diamondoids from Hypercarb HPLC fractions by preparing super-saturated solutions in acetone. Crystallization vials (standard GC-MS autosampler vials) were sealed for approximately one to two weeks after which a small hole was made in the caps and the solvent allowed to evaporate. The crystals were harvested and submitted for structural determination by X-ray crystallography. Fig. S1

shows [1(2,3)4] pentamantane (structure 7 in Fig. 3 in the paper) grown using this method.

Fig. S1. Photomicrographs of [1(2,3)4] pentamantane crystals used for X-ray crystallography. Field of view, approx. 3.5 mm. Photograph, Marilyn Olmstead, U. C. Davis.

⇒ grow crystals for x-ray diffraction

⇒ structural analysis

Cambridge Structural Database entry → One example, huge data base

CCDC FIZ Karlsruhe Leibniz Institute for Information Infrastructure

CSD Entry: GUTDAA

Sign In

Licensed to: Paul Scherrer Institute (PSI)

Simple Search | Structure Search | Unit Cell Search | Formula Search

Your query was: Compound name: pentamantane and the search returned 6 records.

Back to Search List | Modify Search | New Search

Results

Database Identifier	Deposition Number
GUTDAA	198851

Download

GUTDAA : (12(3)4)Pentamantane

Space Group: P $2_1/n$ (14), **Cell:** *a* 7.7105(9)Å *b* 27.040(3)Å *c* 8.9375(10)Å, *α* 90° *β* 115.121(4)° *γ* 90°

3D viewer

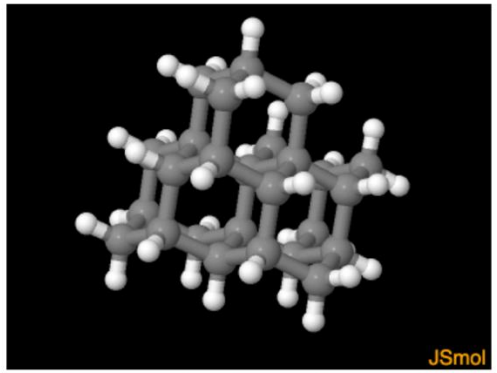

H | Disorder | Menu | Open

Style: Ball and Stick | Labels: No Labels | Packing: None | Measure: None

Chemical diagram

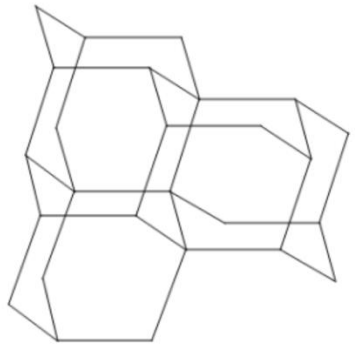

View group symbols key

files for use

Additional details

Deposition Number	198851
Data Citation	J.E.Dahl, S.G.Liu, R.M.K.Carlson CCDC 198851: Experimental Crystal Structure Determination, 2003, DOI: 10.5517/cc6nxk9
Deposited on	29/11/2002

Associated publications

J.E.Dahl, S.G.Liu, R.M.K.Carlson, *Science*, 2003, 299, 96, DOI: 10.1126/science.1078239

Chemical details

Formula	$C_{26}H_{32}$

Crystal details

Space group	P $2_1/n$ (14)
Unit cell	***a*** 7.7105(9)Å ***b*** 27.040(3)Å ***c*** 8.9375(10)Å ***α*** 90° ***β*** 115.121(4)° ***γ*** 90°
Cell volume	1687.14
Reduced cell	***a*** 7.711Å ***b*** 8.938Å ***c*** 27.040Å ***α*** 90.000° ***β*** 90.000° ***γ*** 115.121°
Z, Z'	4, 1
Habit	needle
Colour	colorless

Experimental details

R-factor (%)	5.23
Temperature (K)	90
Density (CCDC)	1.356
Radiation probe	x-ray
Experiment type	single crystal

→ confidence

how structure was determined

https://www.ccdc.cam.ac.uk/structures/Search?Compound=pentamantane&DatabaseToSearch=Published

A real world example: Crystal structure of the Novir Drug

Crystalline structure of (drug) compounds determines

- Melting properties
- Hygroscopicity
- Hydrate formation
- Soluablility
- And other properites

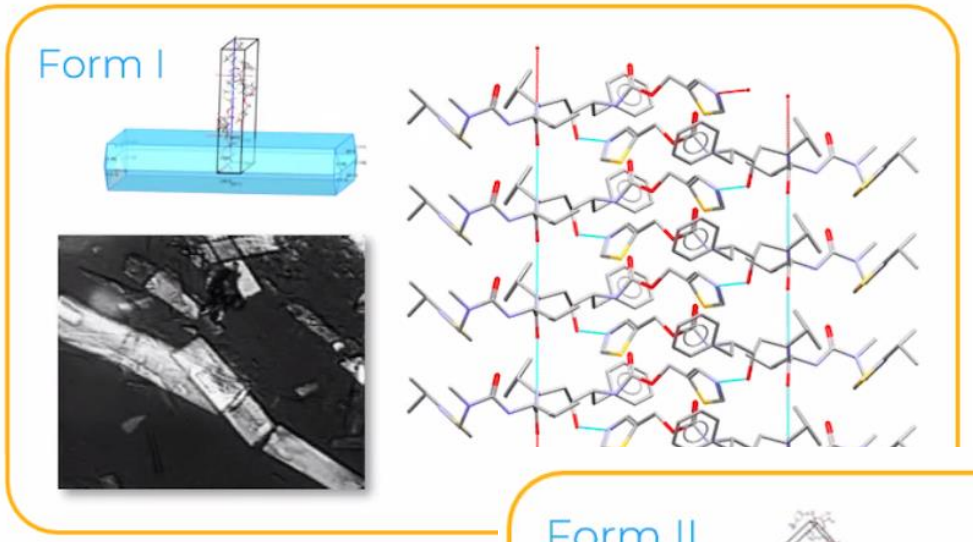

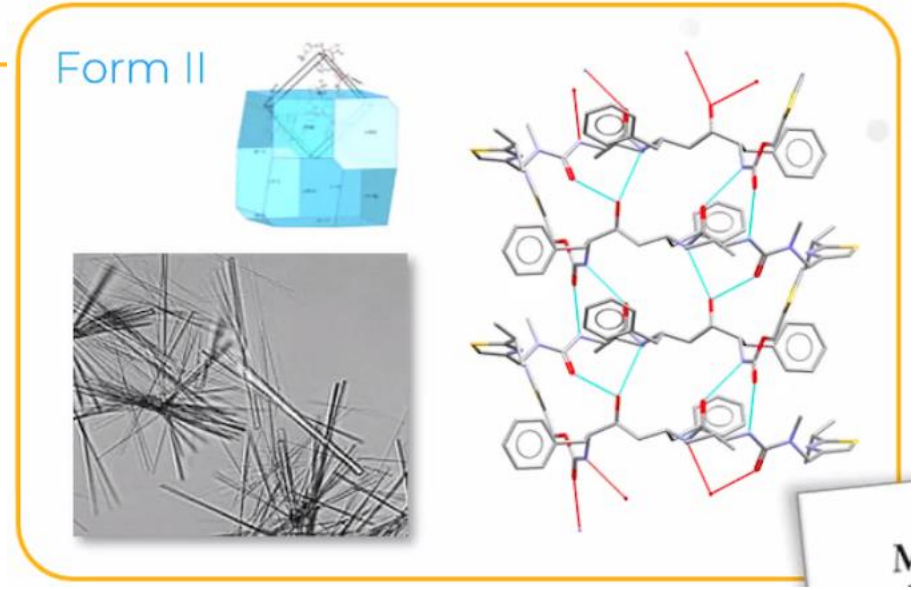

Ritonavir: antiviral drug / HIV drug

(crystal) ⇒ structure very important for function!

Acknowledgement: Susan Reutzel-Edens, CCDC – EPFL PChem Seminar Fall 2021

A real world example: Crystal structure of the Novir Drug

Science news:

› Pharm Res. 2001 Jun;18(6):859-66. doi: 10.1023/a:1011052932607.

Ritonavir: an extraordinary example of conformational polymorphism

J Bauer [1], S Spanton, R Henry, J Quick, W Dziki, W Porter, J Morris

Affiliations + expand

PMID: 11474792 DOI: 10.1023/a:1011052932607

Abstract

Purpose: In the summer of 1998, Norvir semi-solid capsules supplies were threatened as a result of a new much less soluble crystal form of ritonavir. This report provides characterization of the two polymorphs and the structures and hydrogen bonding network for each form.

Methods: Ritonavir polymorphism was investigated using solid state spectroscopy and microscopy techniques including solid state NMR, Near Infrared Spectroscopy, powder X-ray Diffraction and Single crystal X-ray. A sensitive seed detection test was developed.

Results: Ritonavir polymorphs were thoroughly characterized and the structures determined. An unusual conformation was found for form II that results in a strong hydrogen bonding network A possible mechanism for heterogeneous nucleation of form II was investigated.

Conclusions: Ritonavir was found to exhibit conformational polymorphism with two unique crystal lattices having significantly different solubility properties. Although the polymorph (form II) corresponding to the "cis" conformation is a more stable packing arrangement, nucleation, even in the presence of form II seeds, is energetically unfavored except in highly supersaturated solutions. The coincidence of a highly supersaturated solution and a probable heterogeneous nucleation by a degradation product resulted in the sudden appearance of the more stable form II polymorph.

Similar articles

Business news:

thepharmaletter

Up to date news for the Pharmaceutical and Biotechnology industries

Abbott Reports Production Problems For Norvir

27-07-1998

Abbott Laboratories has reported that it is having difficultiesmaintaining production of its HIV protease inhibitor Norvir (ritonavir). The problems are related to its capsule formulation of the antiretroviral.

"We have encountered an undesired formation of a Norvir crystalline structure that affects how the capsule form of Norvir dissolves," commented Arthur Higgins, senior vice president for pharmaceutical operations at Abbott. Although the problem has been identified, to date the company has been unable to come up with a solution.

Abbott stressed that capsules already in circulation are not affected, but there will be shortages and an interruption in supply of the product. Given the seriousness of interrupting treatment in highly-active antiretroviral therapy (which could be associated with the development of resistance and ultimately treatment failure), Abbott is planning to manufacture Norvir in a substitute oral solution so that patients on the drug can maintain their supply. It is estimated that 60,000-70,000 people with HIV are taking the drug.

Effect On Full-Year Sales? Abbott had been projecting sales of around $250 million for Norvir in 1998, and as yet it is unclear whether the supply problems will impact this figure. Sales of the drug last year were around $170 million, less than the performance seen with the other protease inhibitors in 1997. Datamonitor says that Merck & Co's Crixivan (indinavir) had sales of $240 million last year, while Agouron's Viracept (nelfinavir) made around $190 million last year, and Roche's Invirase (saquinavir) made over $200 million.

Analyst Hemant Shah of HKS & Co told Reuters that the other protease inhibitors would definitely gain market share at the expense of Norvir, adding that the impact on Abbott's bottom line will depend greatly on the duration of the problem.

Some very basics about diffraction and scattering

Diffraction, a short review

https://physicsforme.com/2012/01/04/teaching-waves-with-google-earth/

- Should be familiar concept
- A wave encountering an object changes its wavefront. Note that this can also be a density change (later more)
- Fundamental properties of all waves with relevant effects from electron microscopy to shaping coastal landscapes
- In optics most commonly known for limiting resolution in optical setups (microscopes)
- But there is much more!

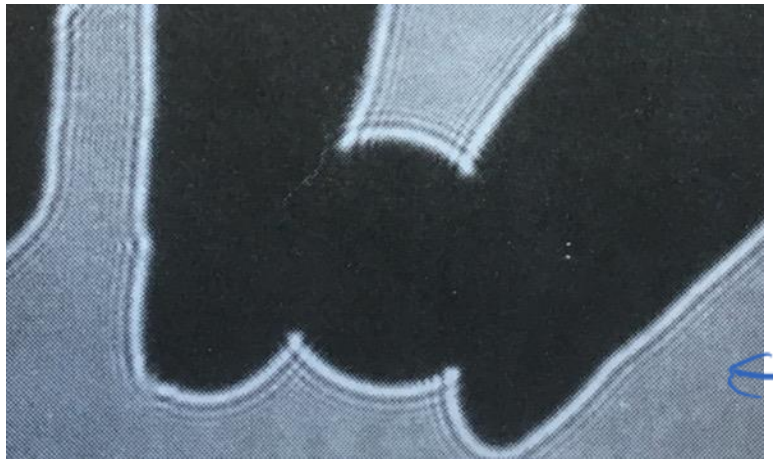

optical microscopy / imaging

The Huygens-Fresnel Principle

- Hugens: every point a wave (a luminous disturbance) reaches becomes a source of a spherical wave; the sum of these secondary waves determines the form of the wave at any subsequent time.
- Huygens-Fresnel: every unobstructed point of a wavefront serves as a source of spherical secondary wavelets. The amplitude of the wave beyond is the superposition of all these wavelets. (includes amplitude and relative phase)

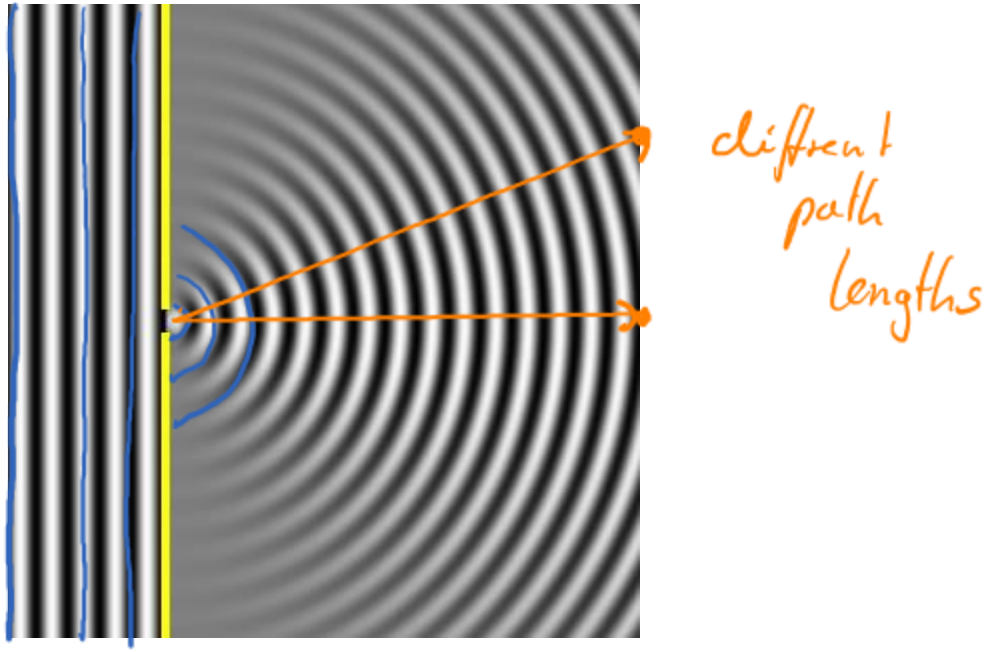

Image credits: By Lookangmany thanks to Fu-Kwun Hwang and author of Easy Java Simulation = Francisco Esquembre - Own work, CC BY-SA 3.0, https://commons.wikimedia.org/w/index.php?curid=16981632

Diffraction from a single slit

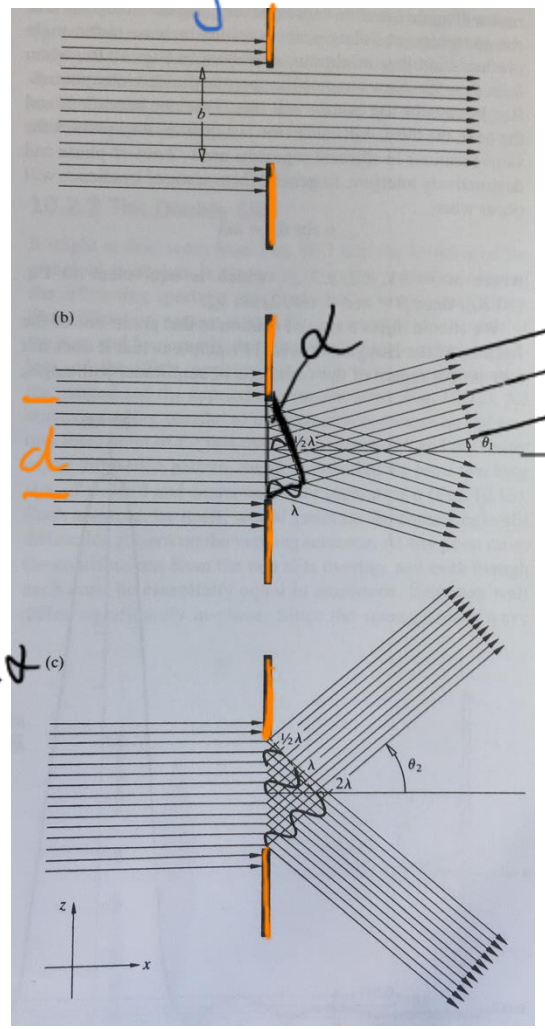

"ray bundles"

pairs above / below center canal

no intensity → min

full intensity → max

α

y

R

d

x

$\frac{x}{d} \approx \sin\alpha$

Min is at $\tan\alpha = \frac{y}{R}$

Destructive interference at $\frac{\lambda}{2} \cdot \frac{2}{d} = \frac{\lambda}{d}$

$\sin\alpha = \frac{\lambda}{d}$; $\sin\alpha \approx \tan\alpha$ for small α

$\Rightarrow \boxed{\frac{y}{R} = \frac{\lambda}{d} \Rightarrow y = n\frac{\lambda}{d} \cdot R \text{ for min}}$

$x \rightarrow$ additional path length for lowest ray $\rightarrow$ here choose λ

The double slit

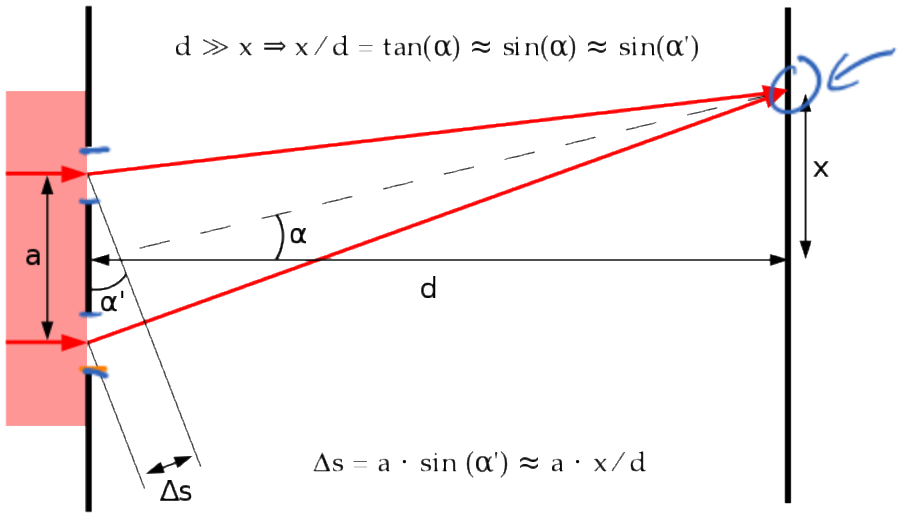

interference condition ↕ geometry

↑ two infinitesimal slits separated by a distance "a"

⇒ hard to treat geometrically by easier in Fourier formalism → Later

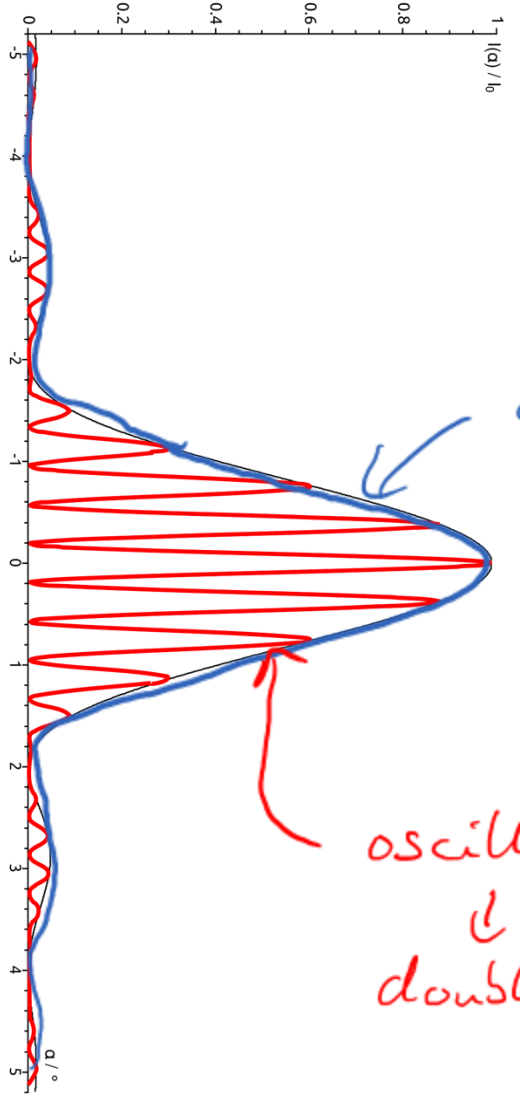

envelope ↓ slit size ↓ single slit

oscillations ↓ double slit

Image source: wikipedia

Diffraction examples

"slits"

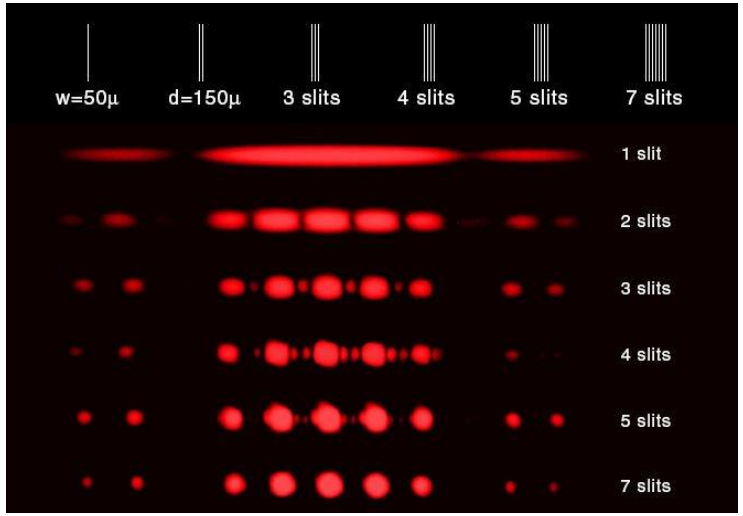

more slits ↓ finer structure

Square aperture

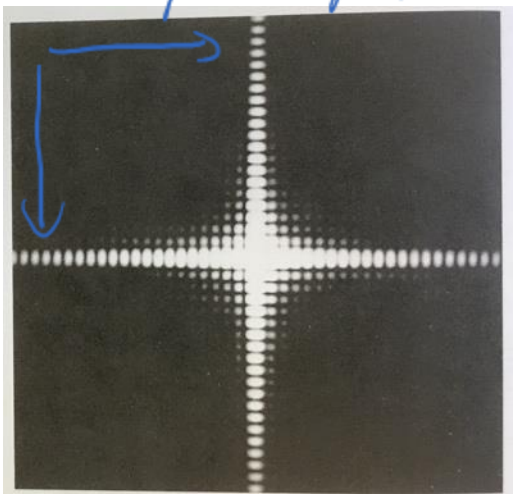

Circular aperture

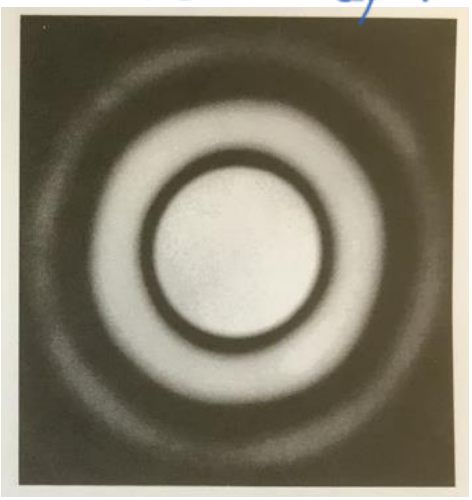

From structure of diffraction pattern, wavelength of light ⇓ structure of sample

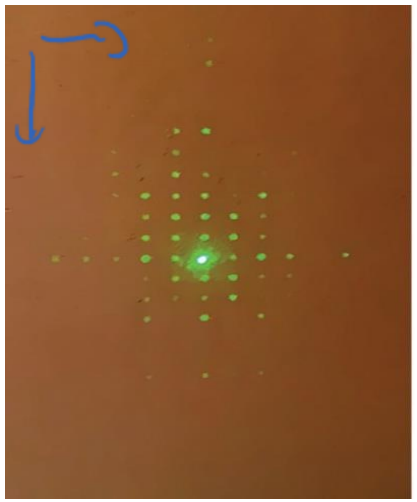

optical light diffraction ⇓ ~ microns ↓ pattern of iphone pixel screen

Watson, Crick → Structure model

Rosalind Franklin → X-ray data of DNA

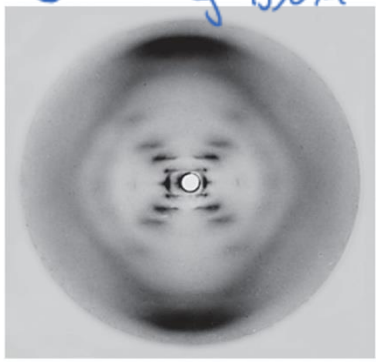

Crystaline materials are characterized by the long-range order

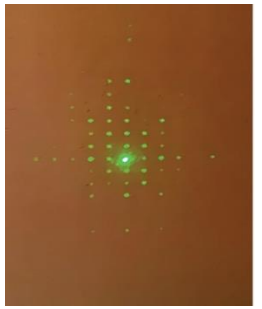

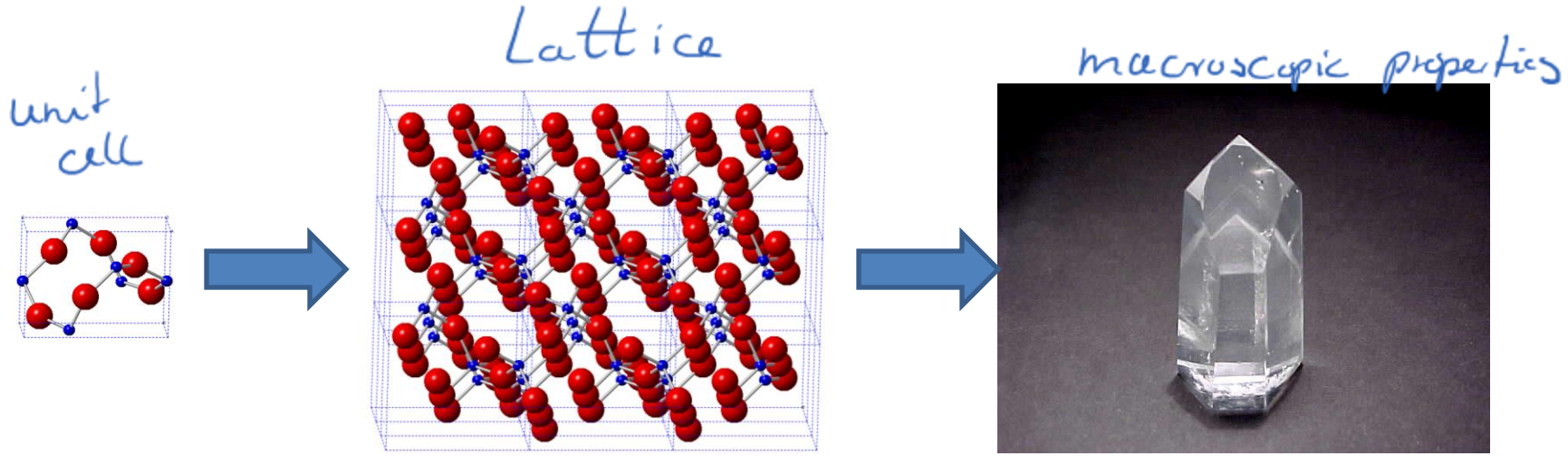

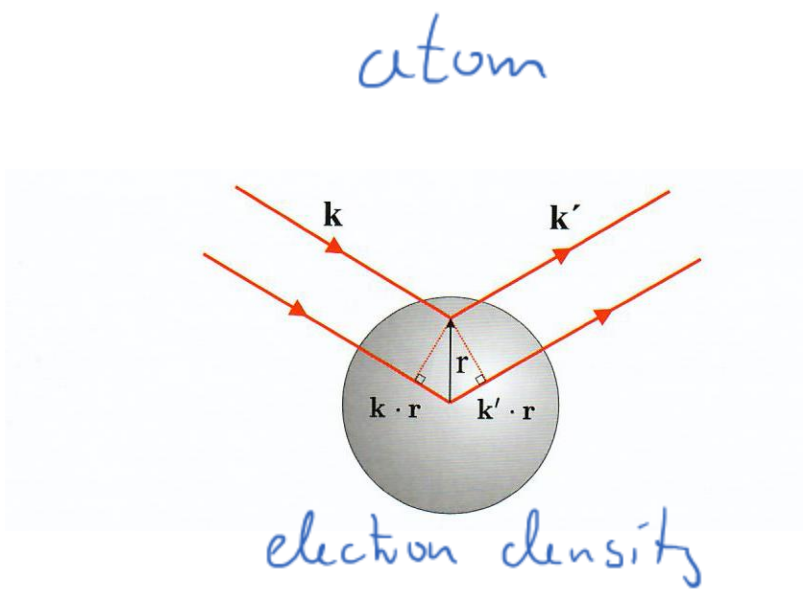

Bragg scattering

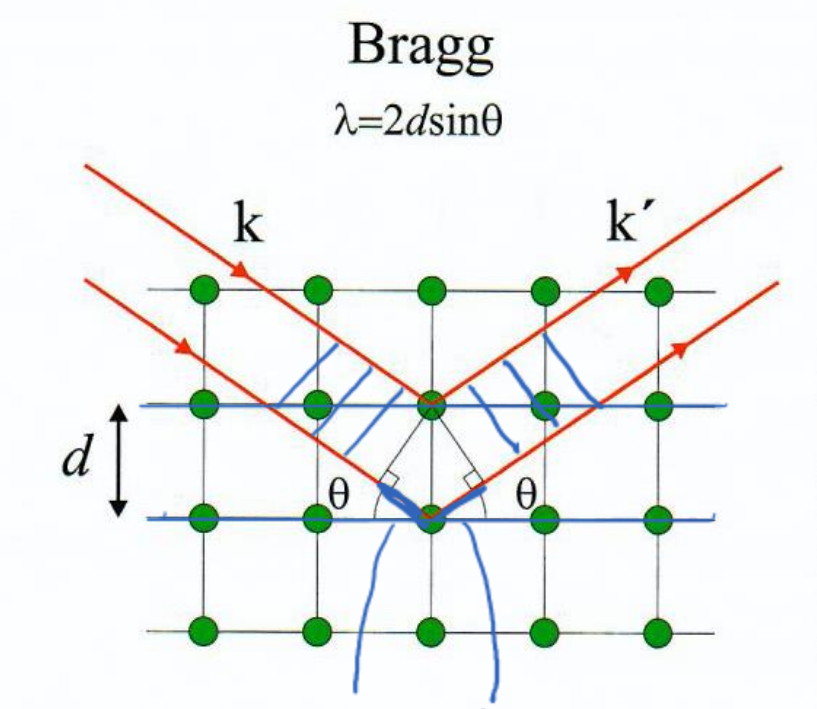

$d \cdot \sin\theta + d \sin\theta$
extra path length

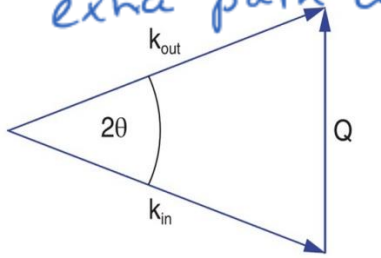

→ atoms in defined positions

→ defined crystal planes

→ x-rays can "reflect" from these planes

The Nobel Prize in Physics 1915

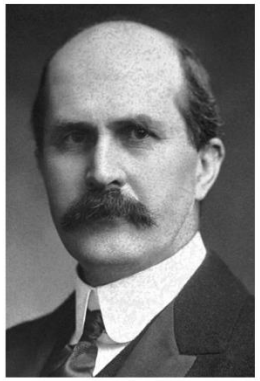

Photo from the Nobel Foundation archive.
Sir William Henry Bragg
Prize share: 1/2

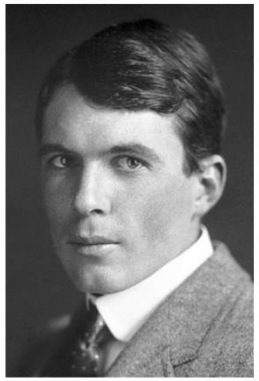

Photo from the Nobel Foundation archive.
William Lawrence Bragg
Prize share: 1/2

Main idea again: exploit interference phenomena

Constitute positive interference

$$\lambda = 2d \sin\Theta$$

$$\sin\Theta = \frac{n\lambda}{2d} \Rightarrow \boxed{2d \sin\Theta = n\lambda}$$

Bragg law

Note: similar formalism applies to many other sample systems

Lattice planes

→ We need formalism to describe Lattice planes

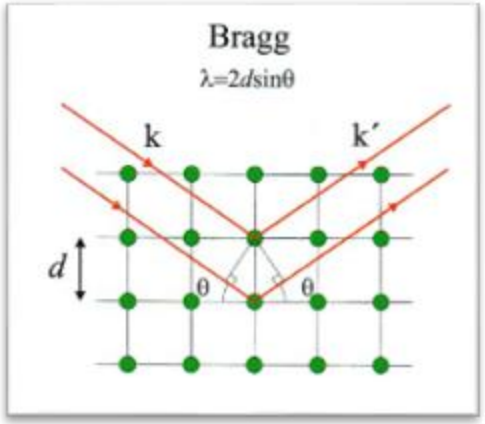

① Look where plane intersects axis

② Take inverse number & reduce to smallest integer number

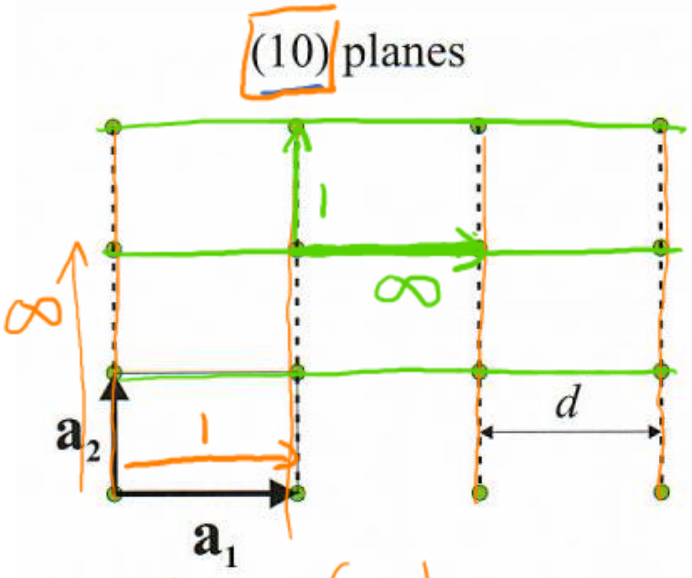

$\frac{1}{1}, \frac{1}{\infty}$ → (10) plane

$\frac{1}{\infty}, \frac{1}{1}$ → (01) plane

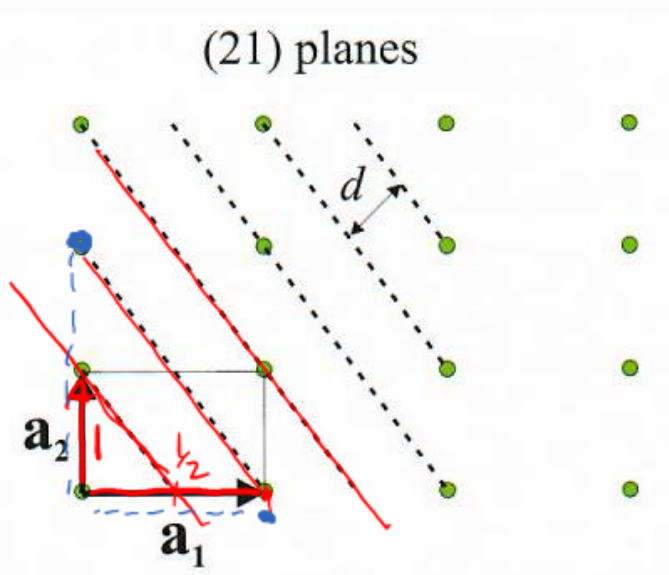

$\frac{1}{½}, \frac{1}{1}$ → (21) plane

or

$\frac{1}{1}, \frac{1}{2}$ → (1, 0.5) → (21) integer

Miller indices

→ Common way to describe lattice planes

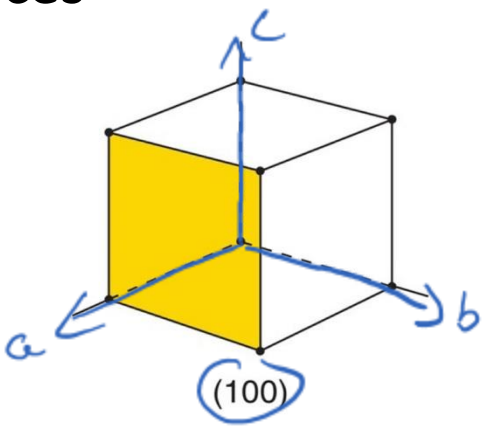

$\frac{1}{1}, \frac{1}{\infty}, \frac{1}{\infty}$

→ (100)

(100)

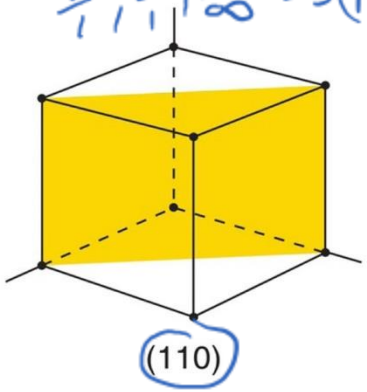

$\frac{1}{1}, \frac{1}{1}, \frac{1}{\infty}$ → (110)

(110)

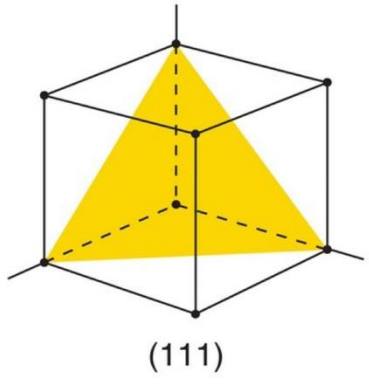

(111)

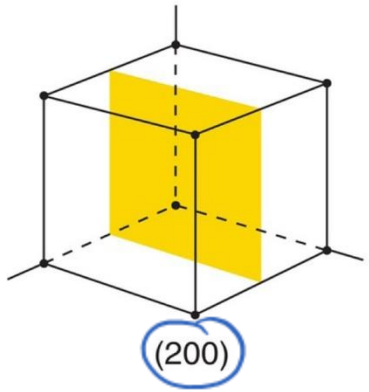

$\frac{1}{\frac{1}{2}}, \frac{1}{\infty}, \frac{1}{\infty}$

→ (200)

(200)

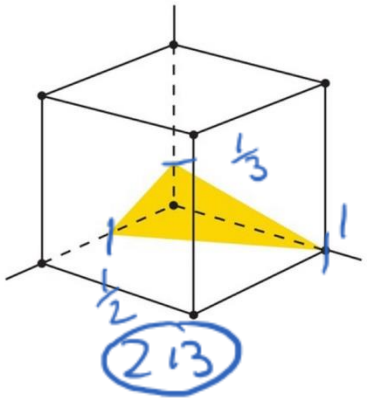

(213)

$\frac{1}{\frac{1}{2}}, 1, 1, \frac{1}{\frac{1}{3}}$

→ (213)

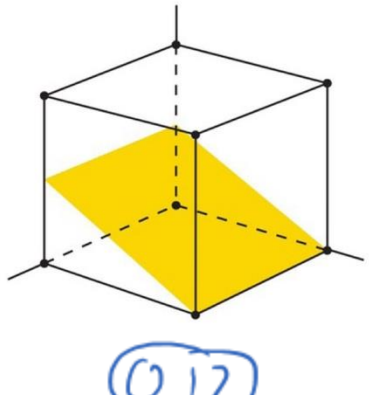

(012)

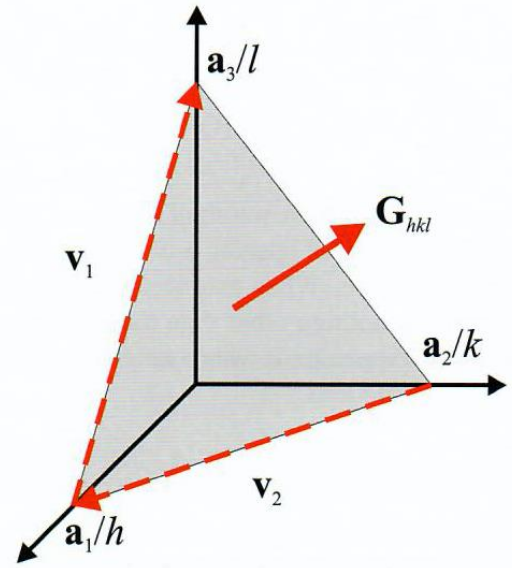

Note already now Miller indices describe vector normal to plane

Recipe:

- find the intercepts of the plane on the respective crystal axis
- take the reciprocal of these numbers, reduce to smallest integer

Exercise: Identify lattice planes

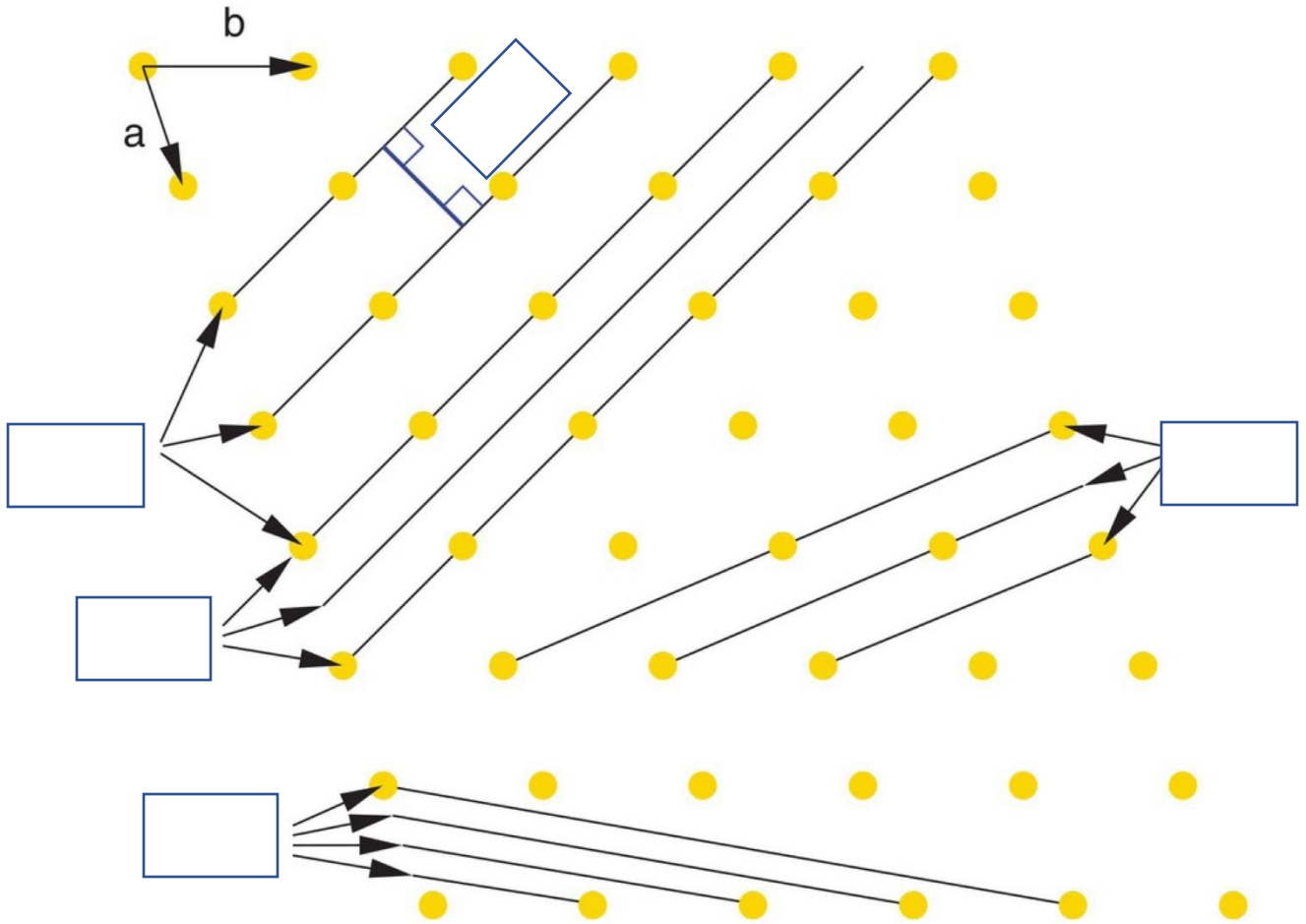

A single crystal (typically) produces one family of Bragg peaks for fixed geometry and λ

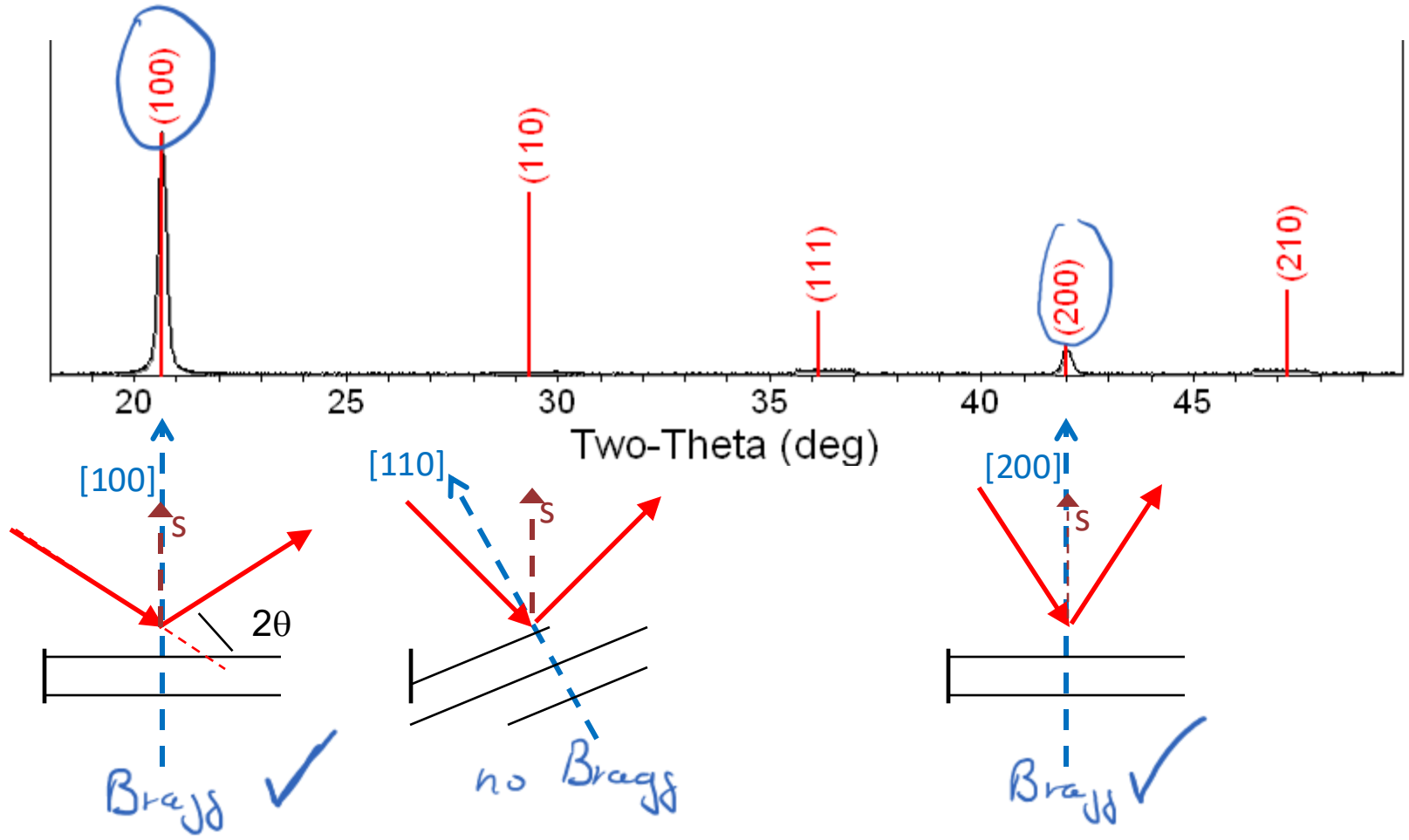

100, 200 parallel → both yield signals but at different angles

If Bragg condition is not met → no constructive interference

Diffraction examples

Diffraction experiment - example

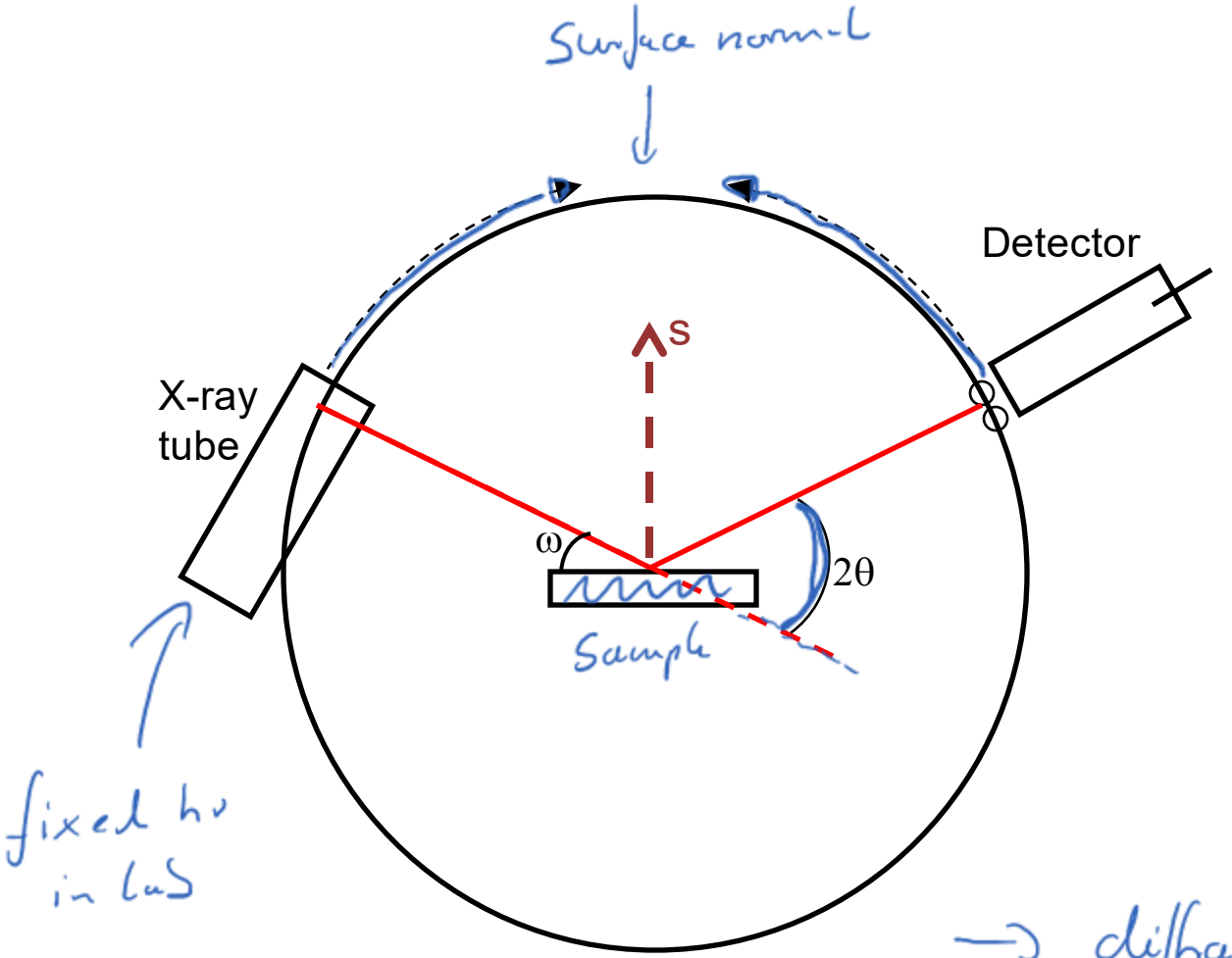

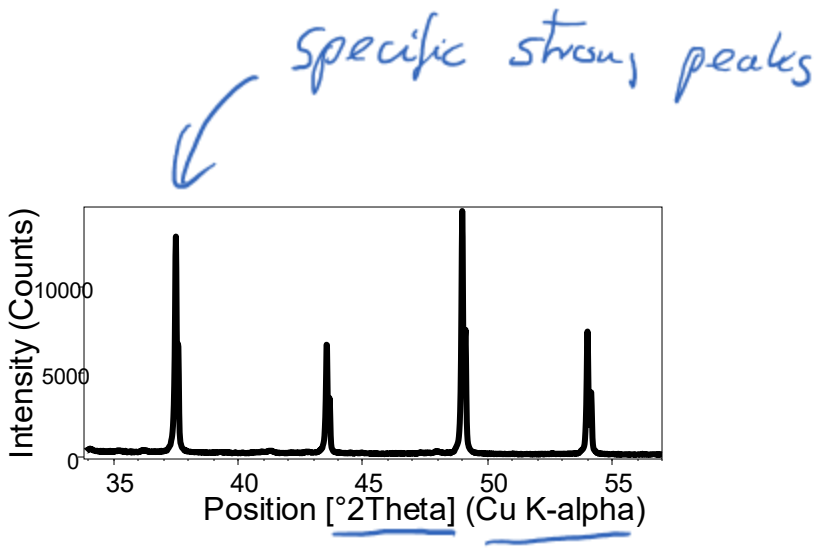

→ diffraction signal

⇕

structure of sample

Characteristic signals from different – chemically identical – samples

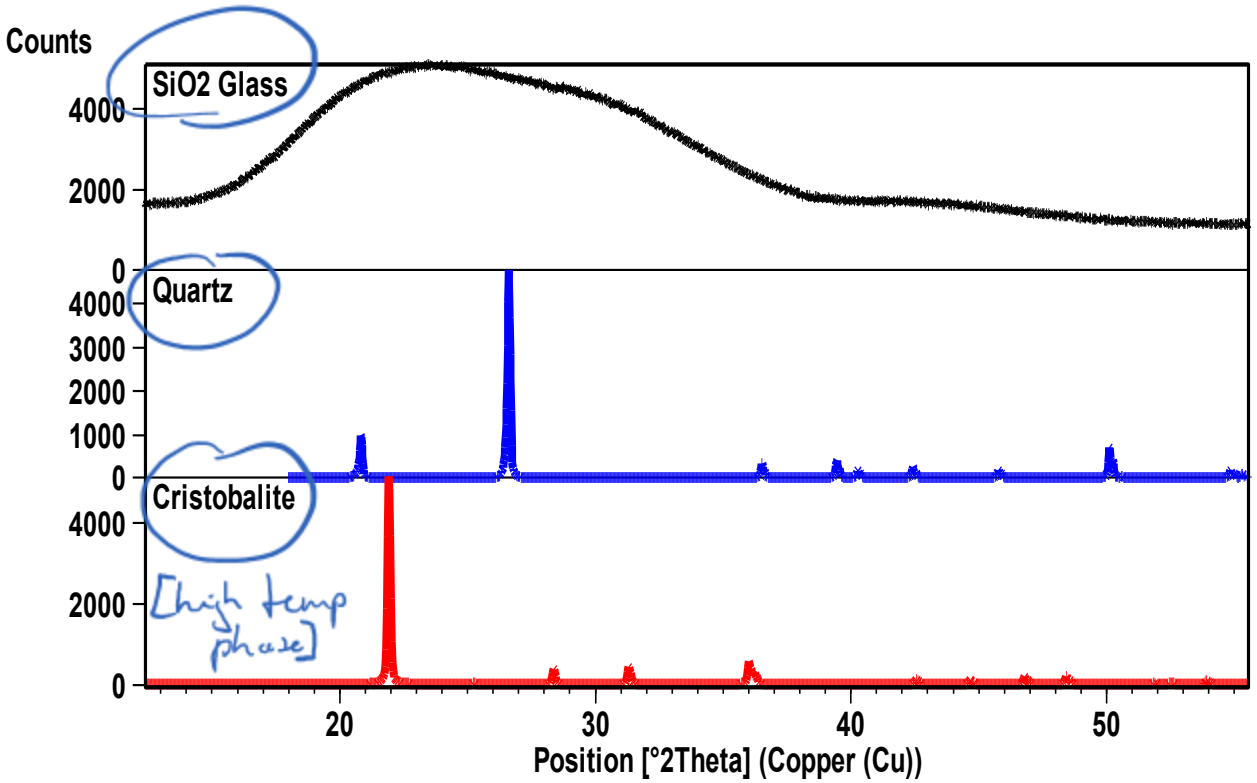

no order (glass)

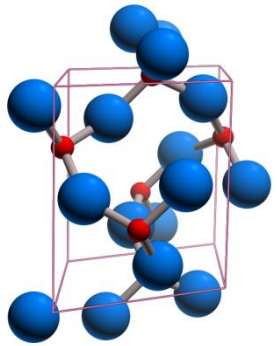

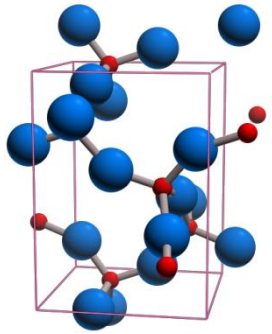

- all SiO_2 samples but different phases
- all structures are chemically identical but their structure order is different

//

XRD yields info about atomic arrangement

The diffraction pattern of a mixture is a simple sum from each component phase

⇒ good analysis tool

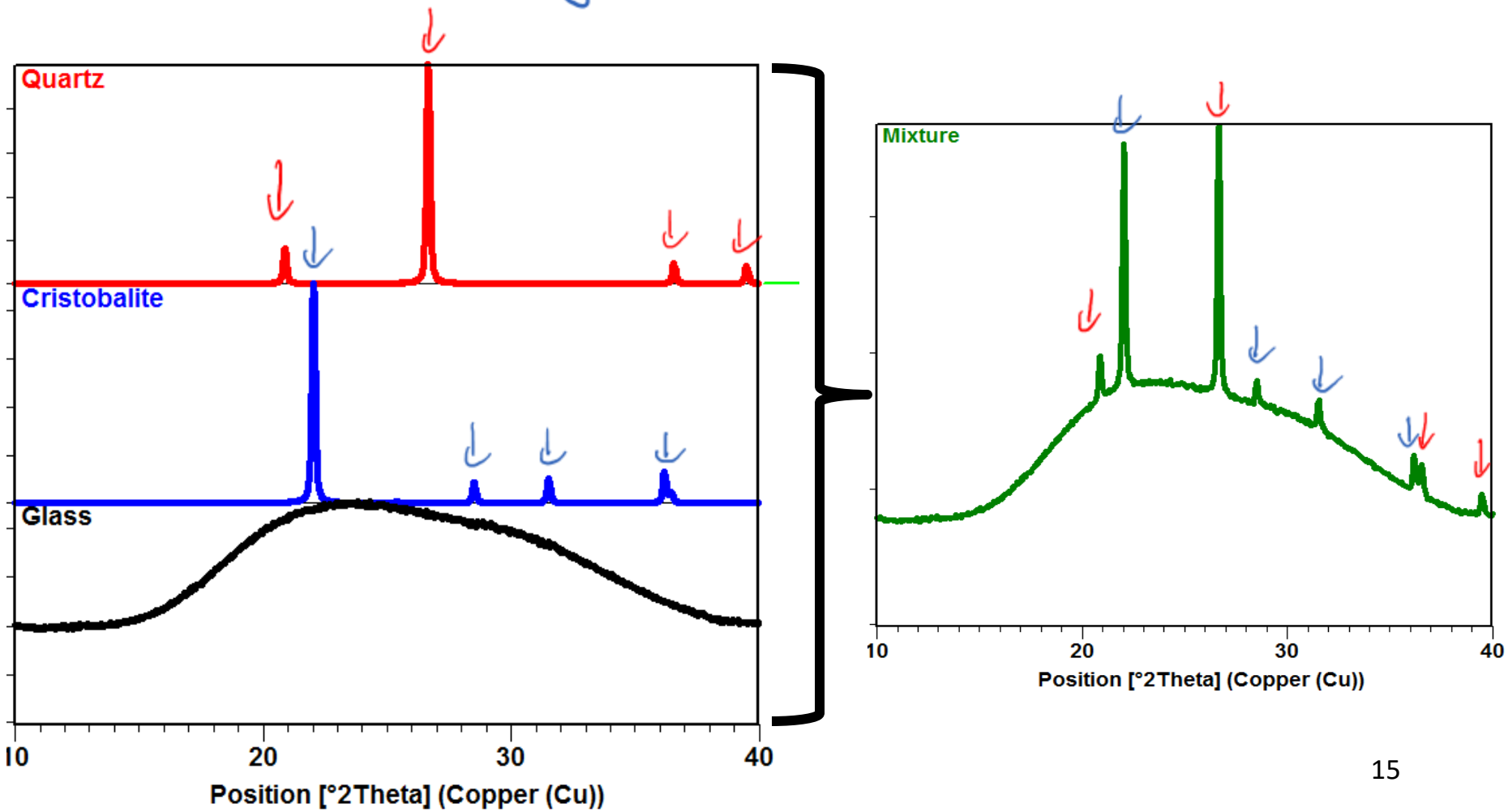

15

Powder diffraction

Diffraction of a polycrystalline sample

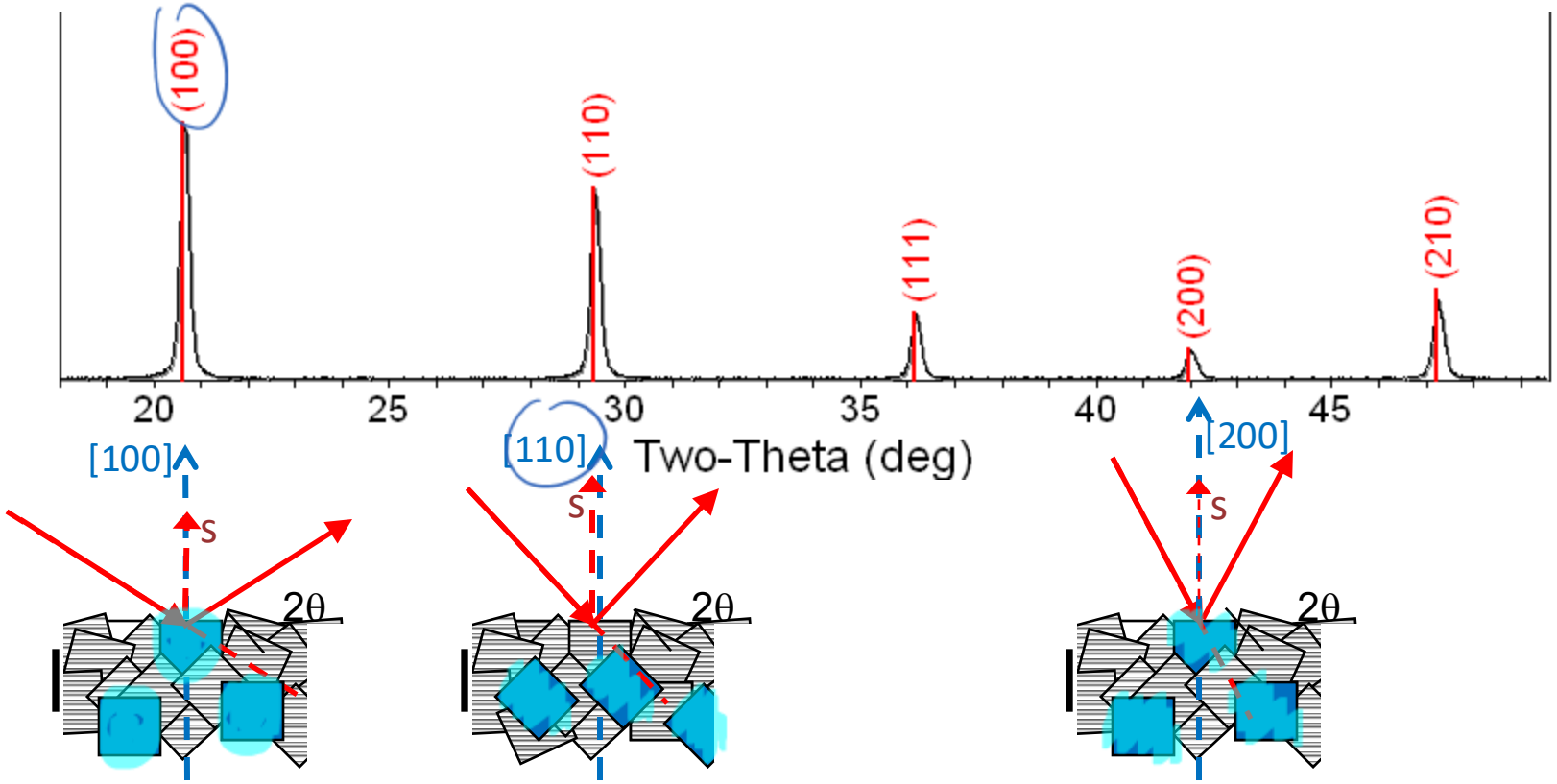

⟹ measure all possible orientations in a statistical average

Diffraction signal of different sample types

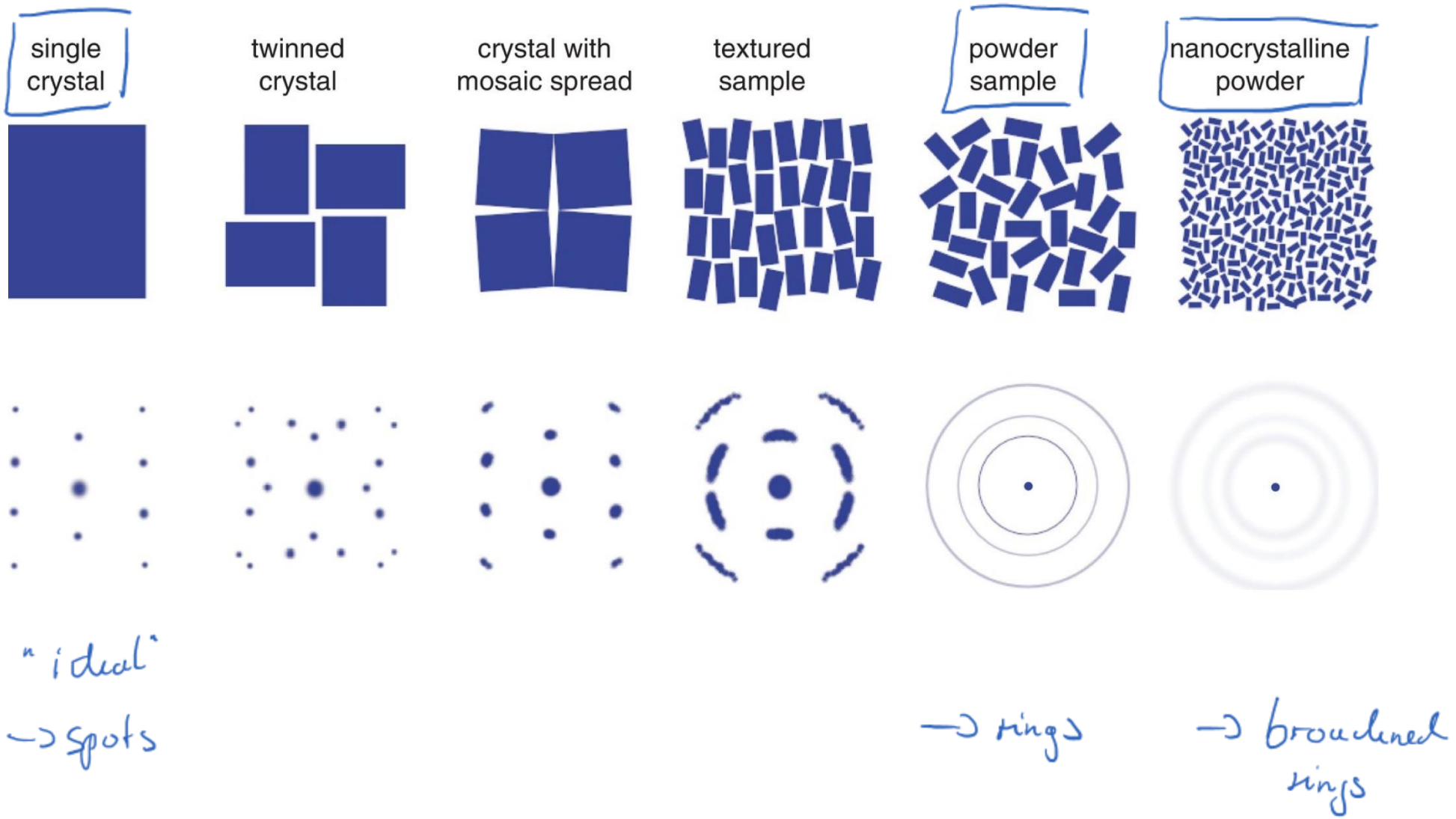

Powder diffraction experiments

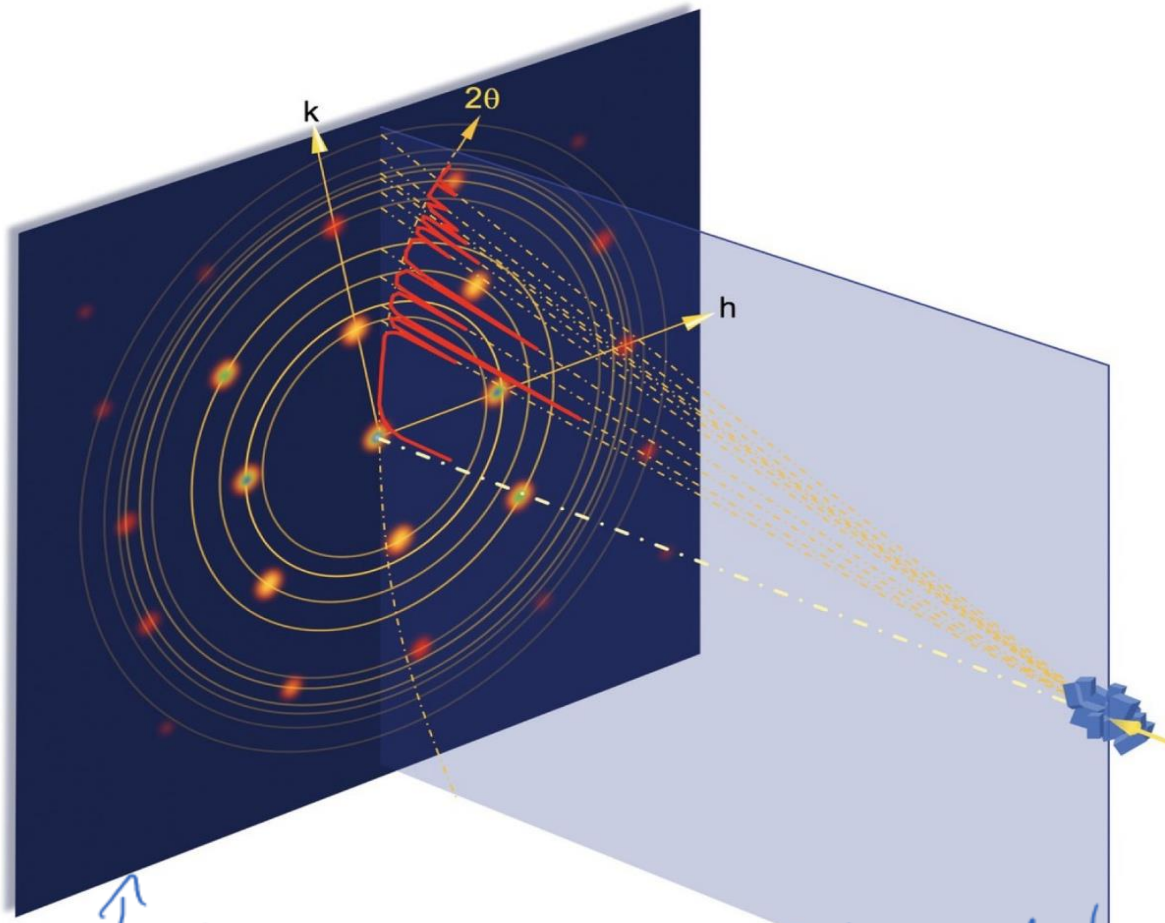

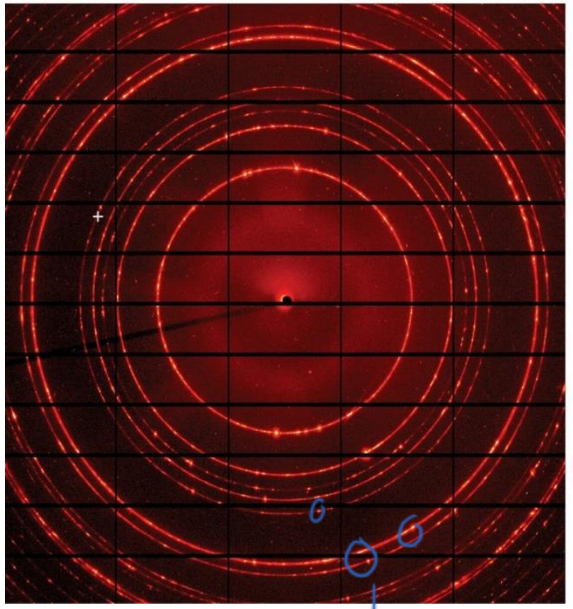

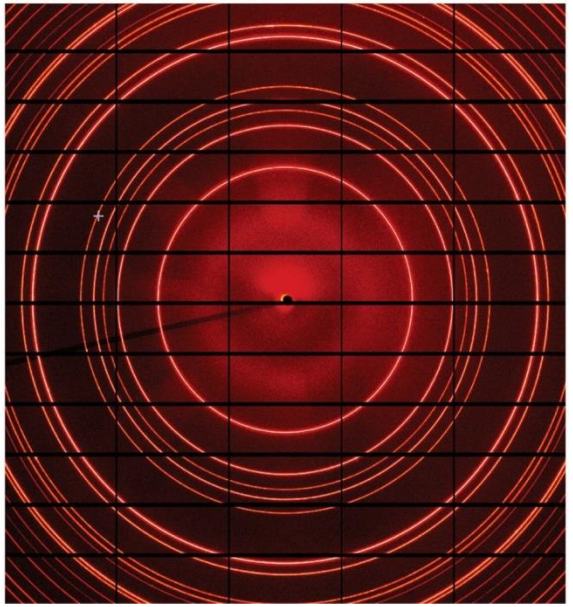

Large crystallites → smooth rings

Shake = average

↑ Bragg angles → powder radial average in 2θ → rings

Use 2D pixel detectors for efficient measurement

Powder diffraction geometry

⇒ Laue diffraction (transmission geometry)

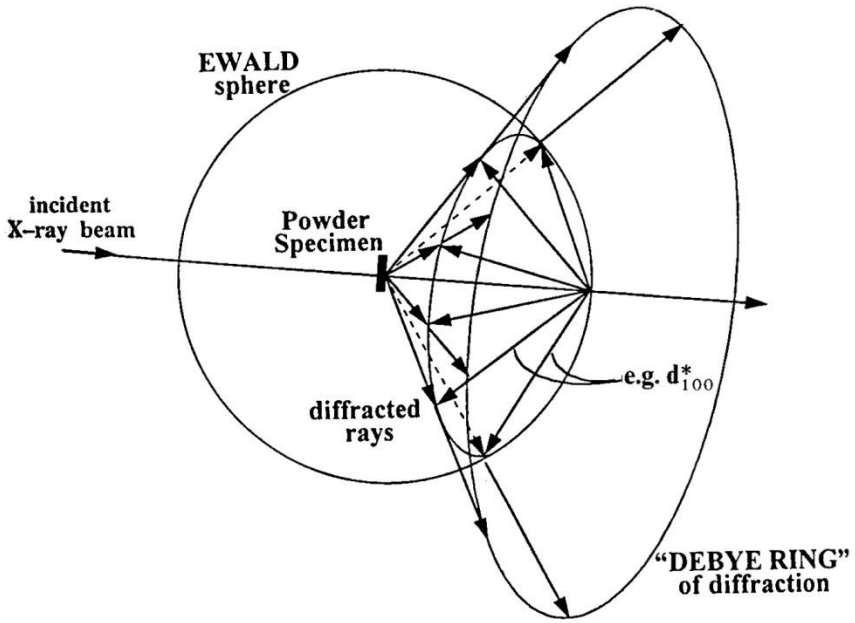

Figure 3.9. The intersection of $\mathbf{d}^*_{100}$ vectors from a powder with the Ewald sphere.

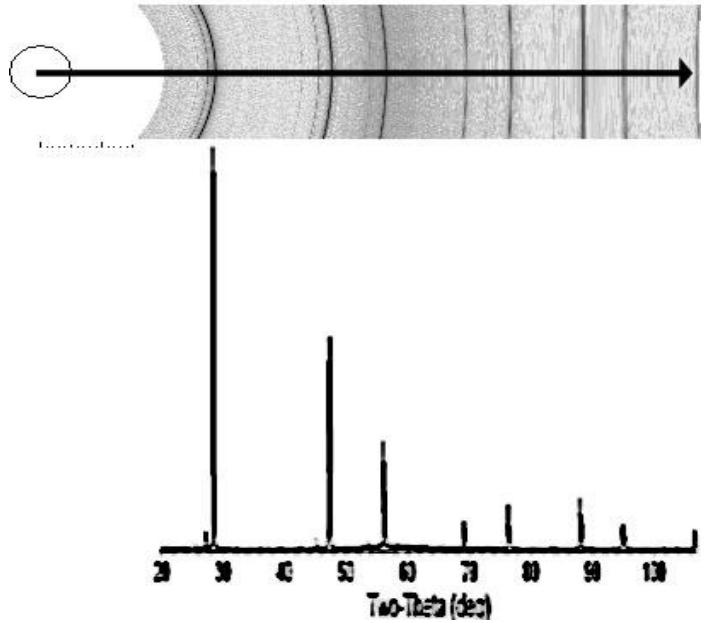

↳ similar to Bragg formalism

↳ transmission geometry

↳ rings in detector plane

↳ earlier: strip detectors, now 2D pixel detectors for efficiency

Powder diffraction data bases for elemental analysis

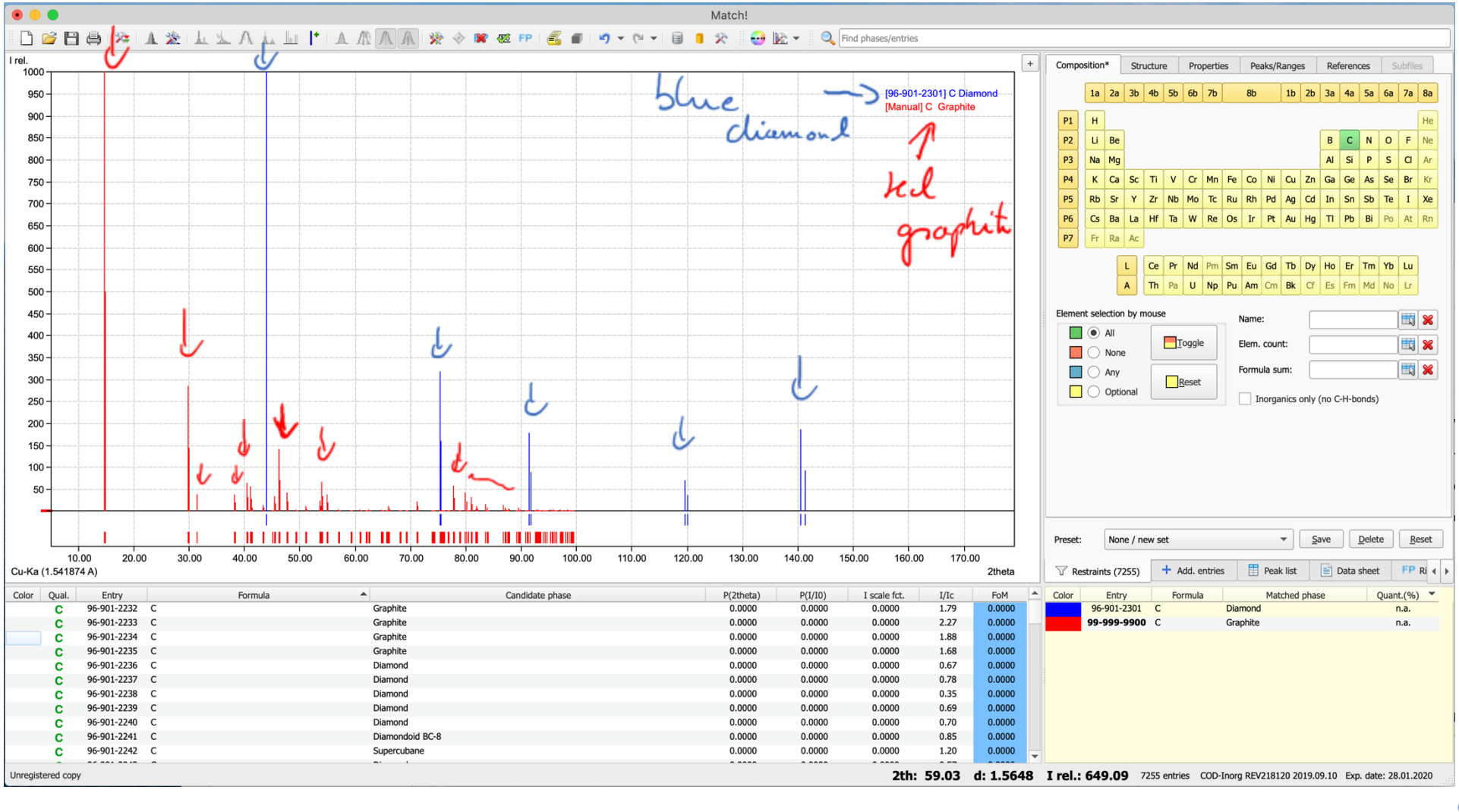

Common tool for structural and phase analysis

||

automated:

feed in your pattern, spits out a structure (proposal)

Debye-Scherrer Formula

The diffraction peak width may contain microstructural information

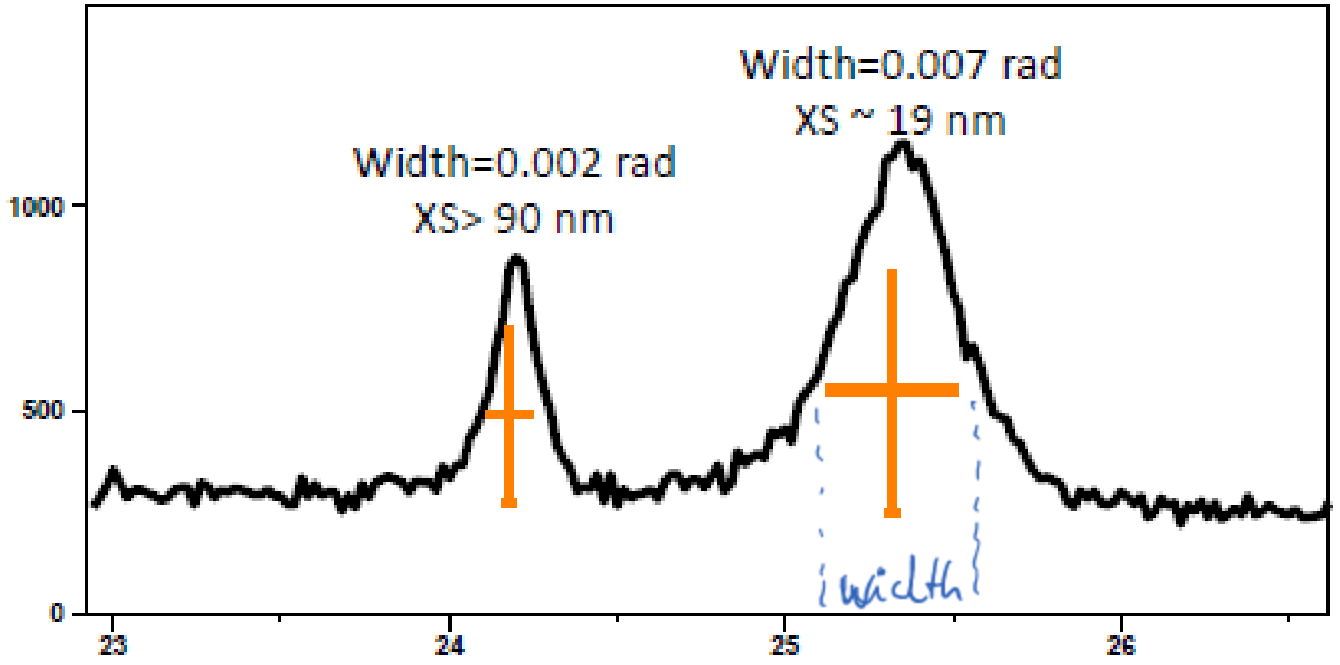

$K \sim 0.9$

$$\text{Size} = \frac{K\lambda}{Width * \cos\theta}$$

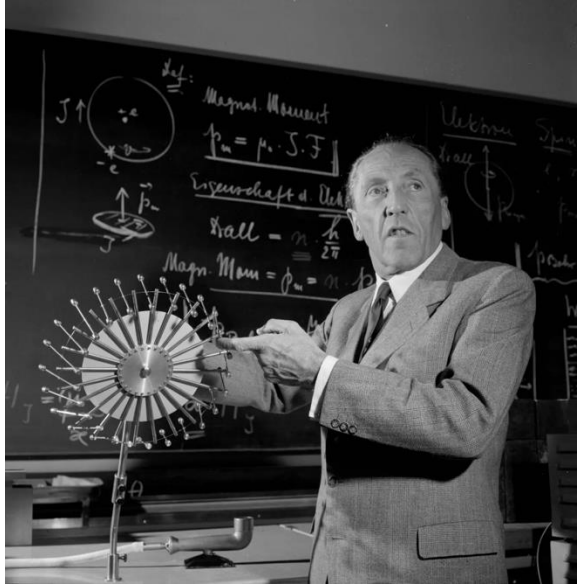

Paul Scherrer
Swiss Physicist (1890-1969)

Note: the "natural" angle are radians

always use

The Debye-Scherrer formula relates the peak width with the particle size

For smaller samples - without the infinite translational symmetry, the peaks are broadened.

Exercise: Colloidal nanoparticles

The diffraction experiments were carried out with a Stoe STADI-P X-ray powder diffractometer at University College London with a Ge(111) monochromator before the sample. A Cu $K\alpha_1$ X-ray beam of wavelength 0.154056 nm was used. The samples were measured in 0.35 mm diameter glass capillaries at room temperature. Capillary diameters were checked to be equal with a micrometer. The diffraction patterns were collected using a position-sensitive

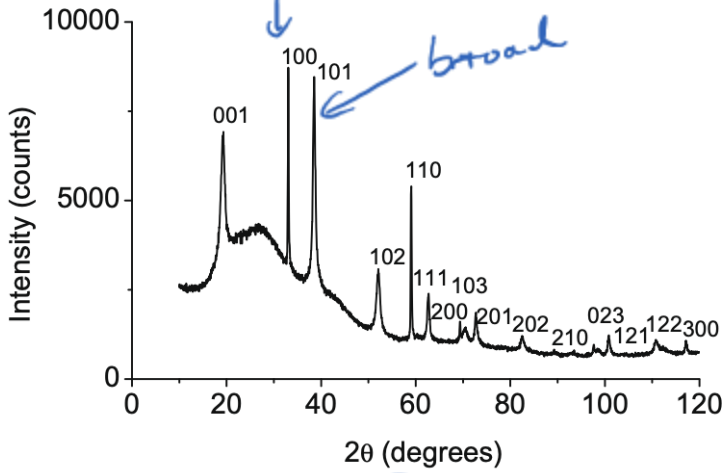

Fig. 1. X-ray diffraction pattern from $Ni(OH)_2$ dispersion $c = 4.610(3)$ Å) with diffraction peaks labeled with *hkl* indice

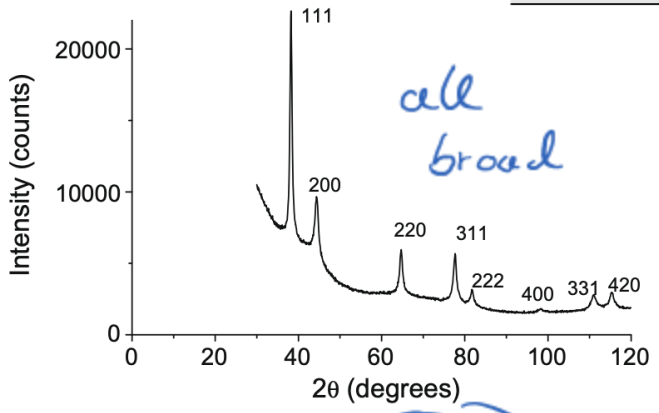

Fig. 2. X-ray diffraction patterns from dispersed Au particles ($a = 4.067(3)$ Å) with diffraction peaks are labeled with *hkl* indices.

Journal of Colloid and Interface Science 338 (2009) 105–110

Contents lists available at ScienceDirect

Journal of Colloid and Interface Science

www.elsevier.com/locate/jcis

Use of wide-angle X-ray diffraction to measure shape and size of dispersed colloidal particles

S. Junaid S. Qazi [a,*], Adrian R. Rennie [a], Jeremy K. Cockcroft [b], Martin Vickers [b]

[a] *Materials Physics, Uppsala University, Ångströmlaboratoriet, Box 530, 75121 Uppsala, Sweden*
[b] *Applied Crystallography Group, Department of Chemistry, University College London, 20 Gordon Street, London WC1H 0AJ, UK*

Table 1
Results from the pseudo-Voigt function fit to the $Ni(OH)_2$ sample. 2θ is the peak position for the Cu $K\alpha_1$ radiation wavelength (0.154056 nm).

hkl	Bragg angle 2θ (°)	Peak width 'β' (°)	Instrument resolution (°)	Corrected β (°)
001	19.25	1.140	0.121	1.02
100	33.06	0.197	0.115	0.08
101	38.52	0.593	0.114	0.48
102	52.06	0.876	0.117	0.76
110	59.05	0.248	0.120	0.13
111	62.67	0.550	0.122	0.43

Table 2
Results from the pseudo-Voigt fit to the Au particles. 2θ is the peak position for the Cu $K\alpha_1$ radiation wavelength (0.154056 nm).

hkl	Bragg angle 2θ (°)	Peak width 'β' (°)	Instrument resolution (°)	Corrected β (°)
111	38.21	0.580	0.114	0.47
200	44.34	0.822	0.115	0.71
220	64.69	0.810	0.123	0.68
311	77.63	0.905	0.135	0.77
420	115.34	1.194	0.119	1.07

A few examples and case studies

Example: EPFL XRD instrument

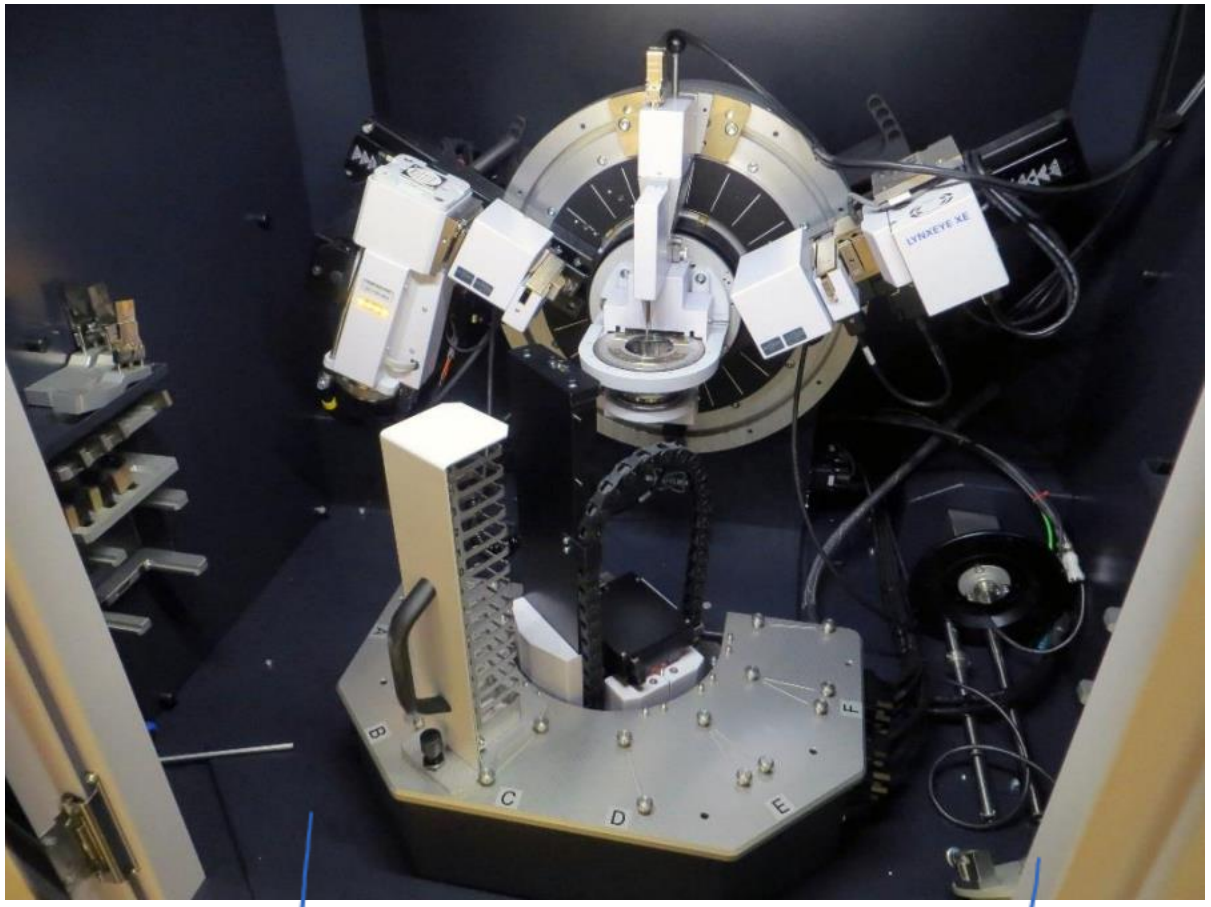

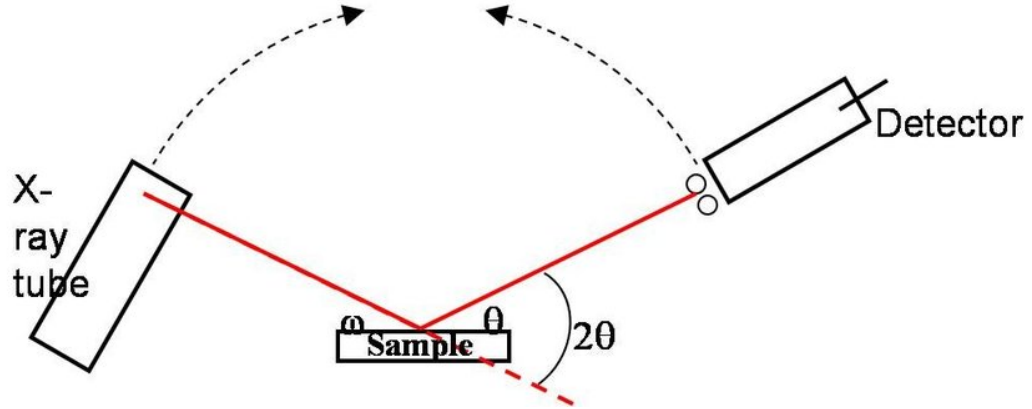

⇒ accessible as tool

⇒ elective courses about XRD

Example Synchrotron Source

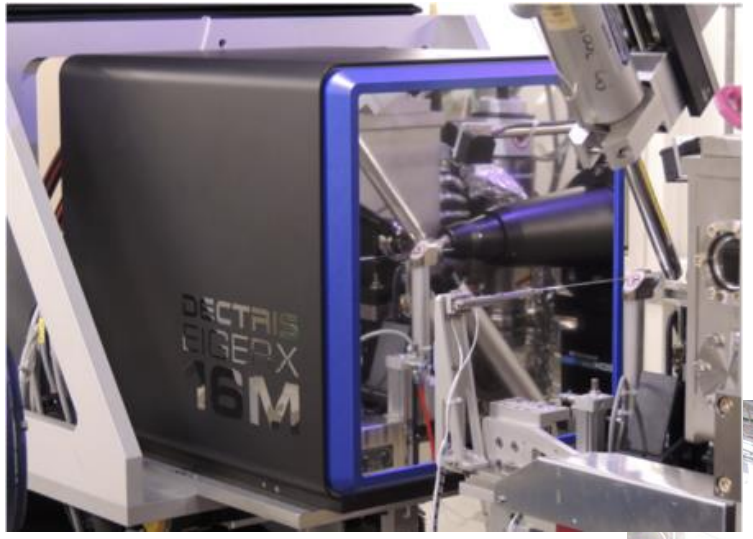

(expensive) area detectors

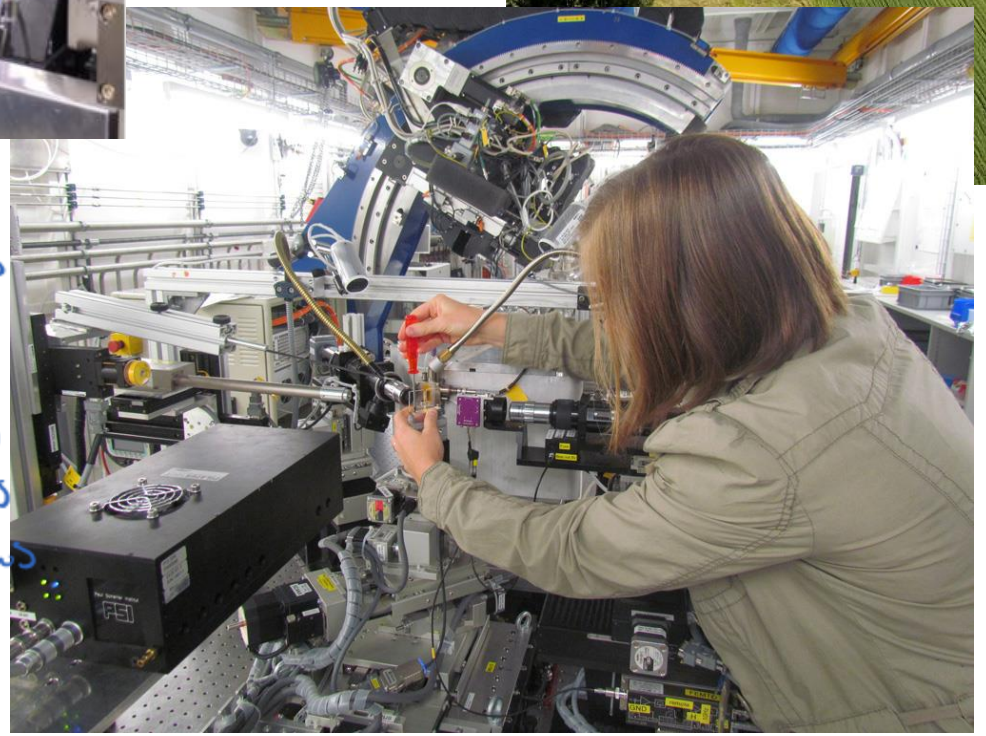

dedicated beamlines for different approaches

Villigen, AG

Many beamlines dedicated to (powder) diffraction.

Example: In-operando battery research

JACS
JOURNAL OF THE AMERICAN CHEMICAL SOCIETY

Article

pubs.acs.org/JACS

In Operando X-ray Diffraction and Transmission X-ray Microscopy of Lithium Sulfur Batteries

Johanna Nelson,[†,‡,⊥] Sumohan Misra,[†,⊥] Yuan Yang,[§,⊥] Ariel Jackson,[§] Yijin Liu,[†] Hailiang Wang,[∥] Hongjie Dai,[∥] Joy C. Andrews,[†] Yi Cui,*[,‡,§] and Michael F. Toney*[,†,‡]

[†]Stanford Synchrotron Radiation Lightsource, and [‡]Stanford Institute for Materials and Energy Science, SLAC National Accelerator Laboratory, 2575 Sand Hill Road, Menlo Park, California 94025, United States

[§]Department of Materials Science and Engineering, and [∥]Department of Chemistry, Stanford University, Stanford, California 94305, United States

→ Motivation: new/alternative battery design

→ Question: what are structural and morphological changes during the electrochemical process

→ Experiment: showed recrystallization of sulfur during charging / also depending how anode material was processed

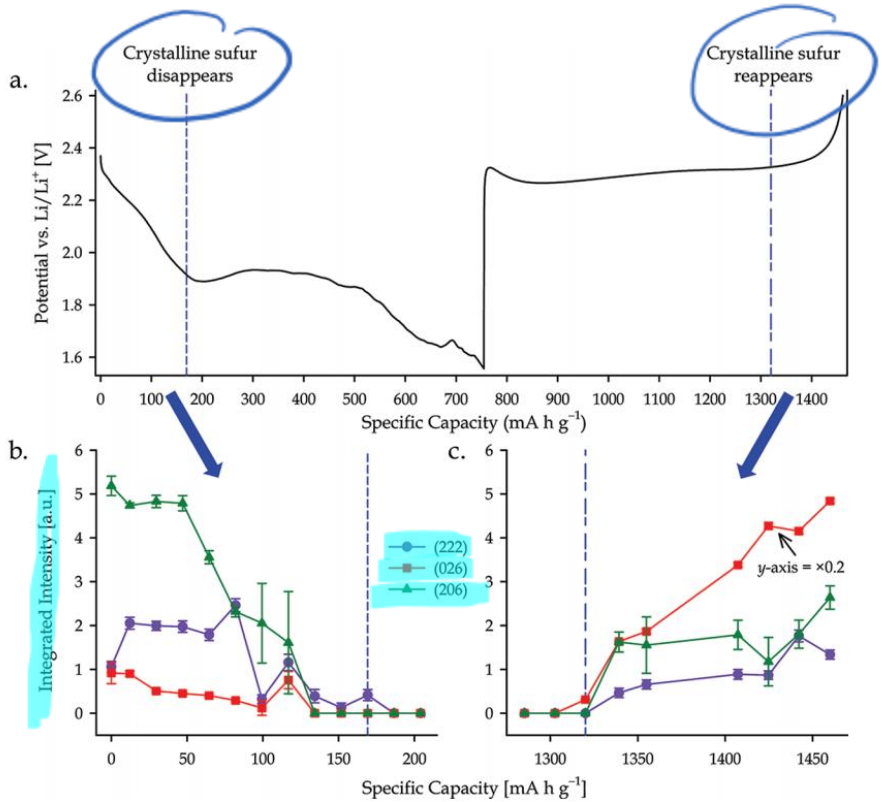

Figure 3. Integrated diffraction intensities of sulfur peaks for a Li–S cell cycled at *C*/8 and with a cathode prepared as a sulfur/Super P composite: (a) electrochemical plot showing the first cycle of the Li–S cell; (b and c) integrated intensity plots for (222), (026) ,and (206) Bragg peaks, which show the disappearance of crystalline sulfur by the end of the first discharge plateau and its reappearance by the end of the charge cycle. The blue arrows indicate the specific capacity regions over which the integrated intensities are plotted. The dashed lines emphasize where sulfur peaks disappear and reappear. The total discharge capacity is 755 mA h g^{-1}, and the total charge capacity is 707 mA h g^{-1}. Error bars on the integrated intensities were determined using Levenberg–Marquardt minimization.

Example: In operando – laser printing PSI

ARTICLE IN PRESS

Materials Today • Volume xxx, Number xx • xxxx 2019 RESEARCH

ELSEVIER

Operando X-ray diffraction during laser 3D printing

Samy Hocine [1,2], Helena Van Swygenhoven [1,2,*], Steven Van Petegem [1], Cynthia Sin Ting Chang [1], Tuerdi Maimaitiyili [1], Gemma Tinti [3], Dario Ferreira Sanchez [4], Daniel Grolimund [4], Nicola Casati [5]

→ Additive manufacturing is a hot topic in materials science / also chemistry

→ What are the processes involved, what phases are created, etc

→ Experiment: Print with laser, follow with X-rays

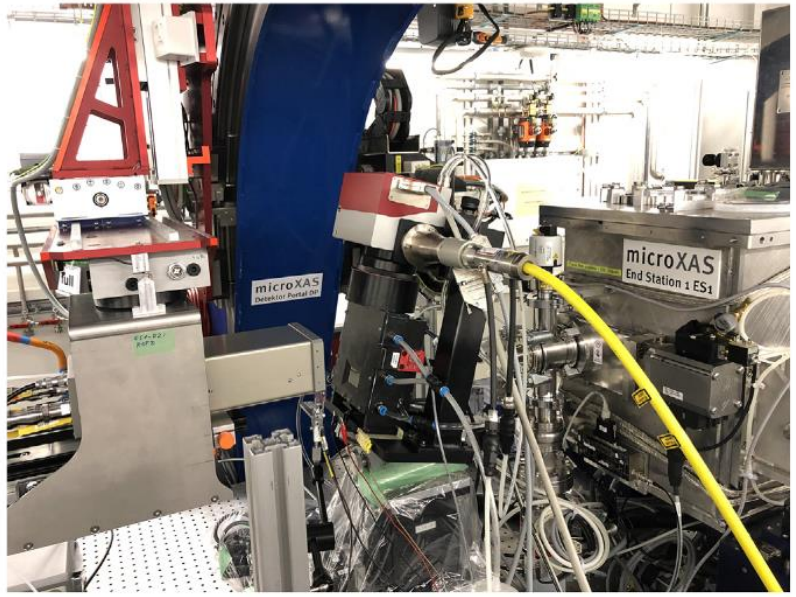

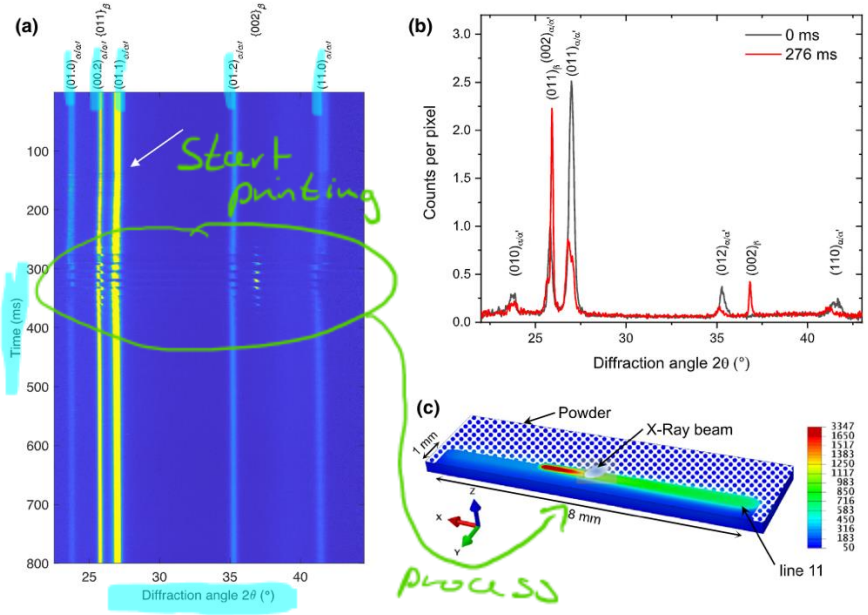

FIGURE 3

(a) Phase evolution during printing of a single layer, shown as an intensity vs. diffraction angle and time by stacking 16,000 individual diffraction patterns. The white arrow indicates the start of the printing process, (b) diffraction patterns recorded prior to printing and during printing of the 11th line at $t = 276$ ms, (c) schematic representation of the relative position of laser, X-ray beam and HAZ at $t = 276$ ms. (Temperature scale in degree Celsius).

Outlook

Diffraction as Fourier Transform

Reciprocal Lattice

Bragg and Laue Diffraction

Structure Factor

Detailed Electronic Structure Maps

Diffraction as Fourier transform:

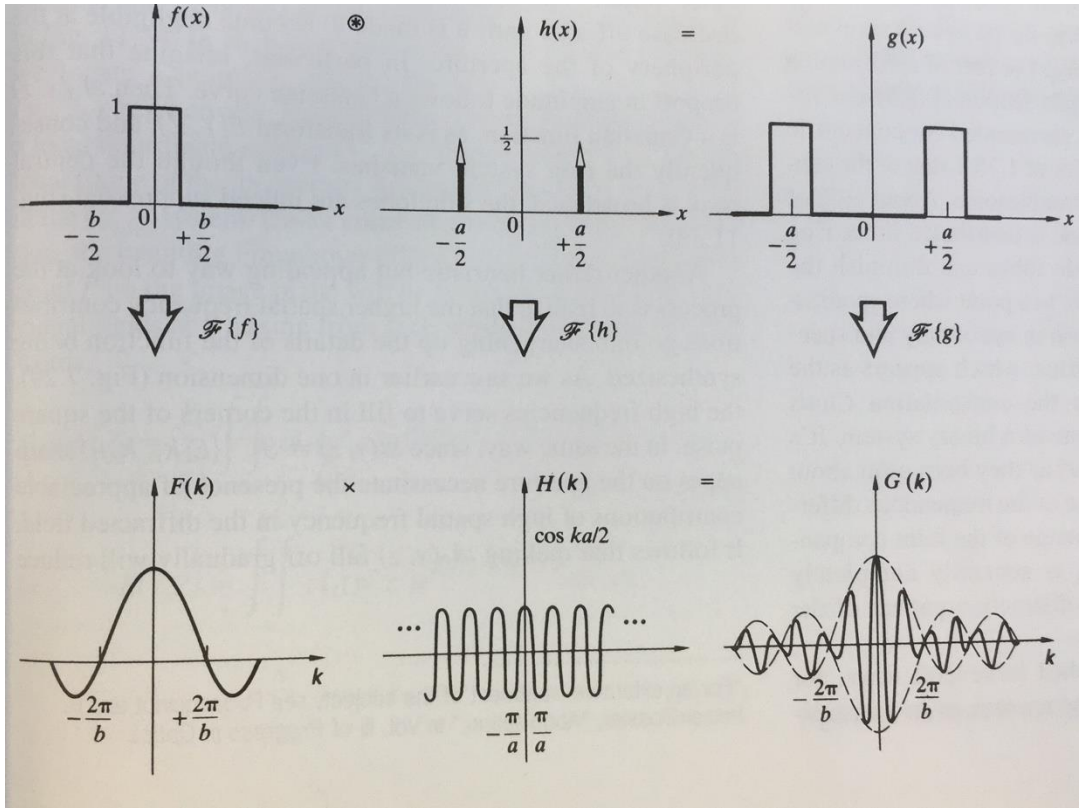

For each lattice a reciprocal lattice can be defined

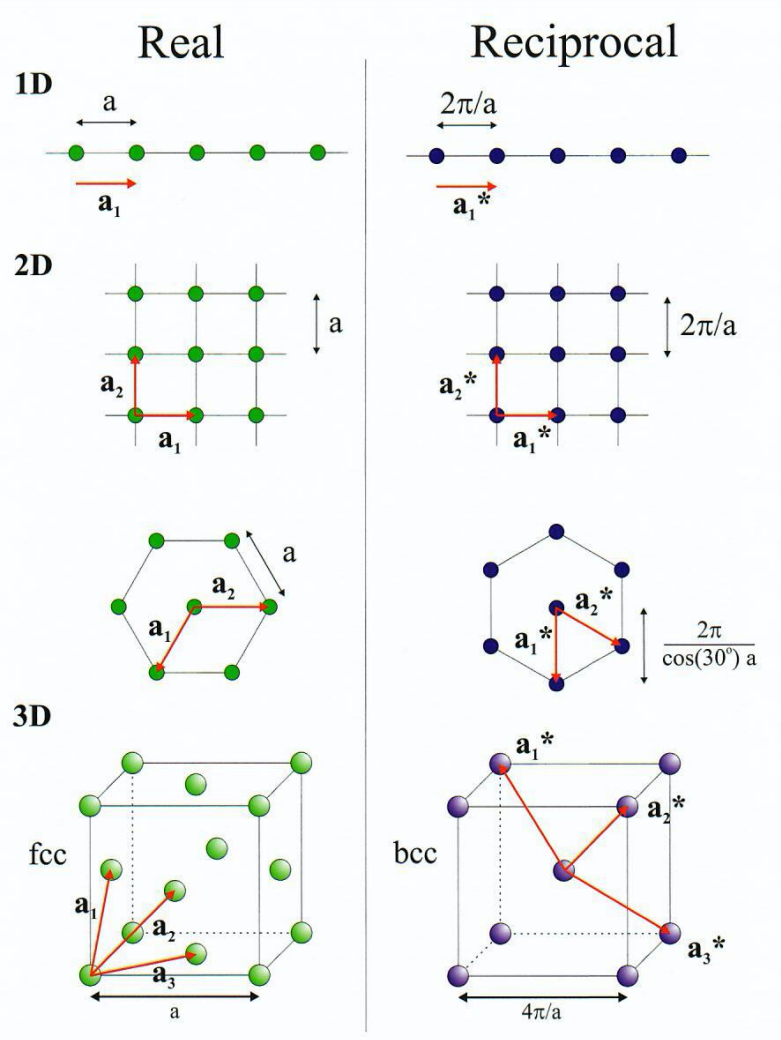

Bargg and Laue conditions

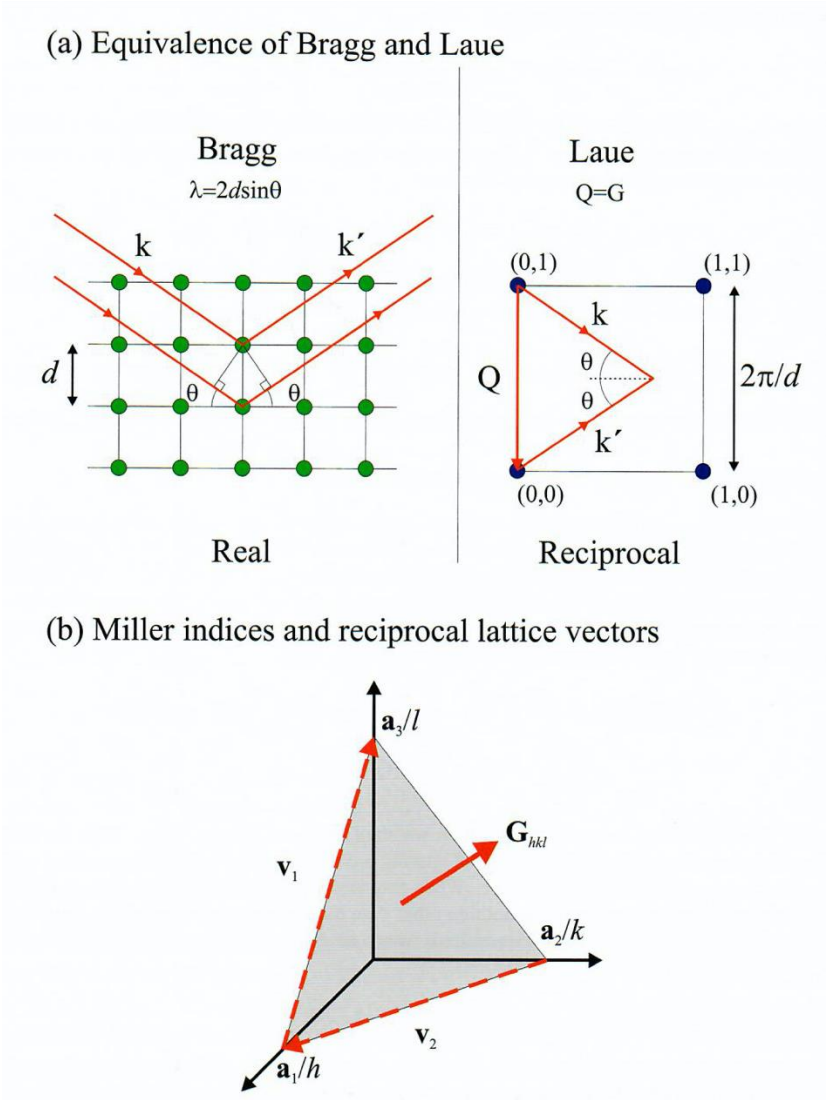

The Nobel Prize in Physics 1914

Photo from the Nobel Foundation archive.

Max von Laue

Prize share: 1/1

A crystal is defined by ist lattice and basis

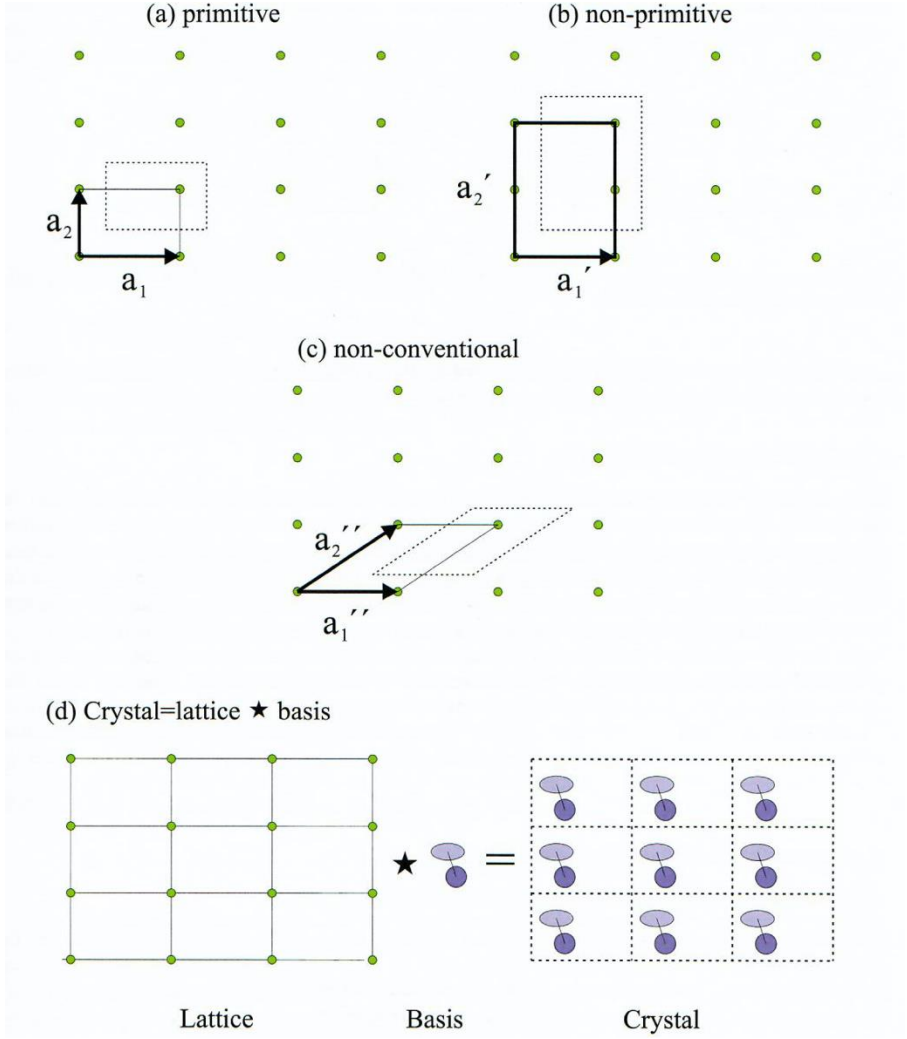

The structure factor

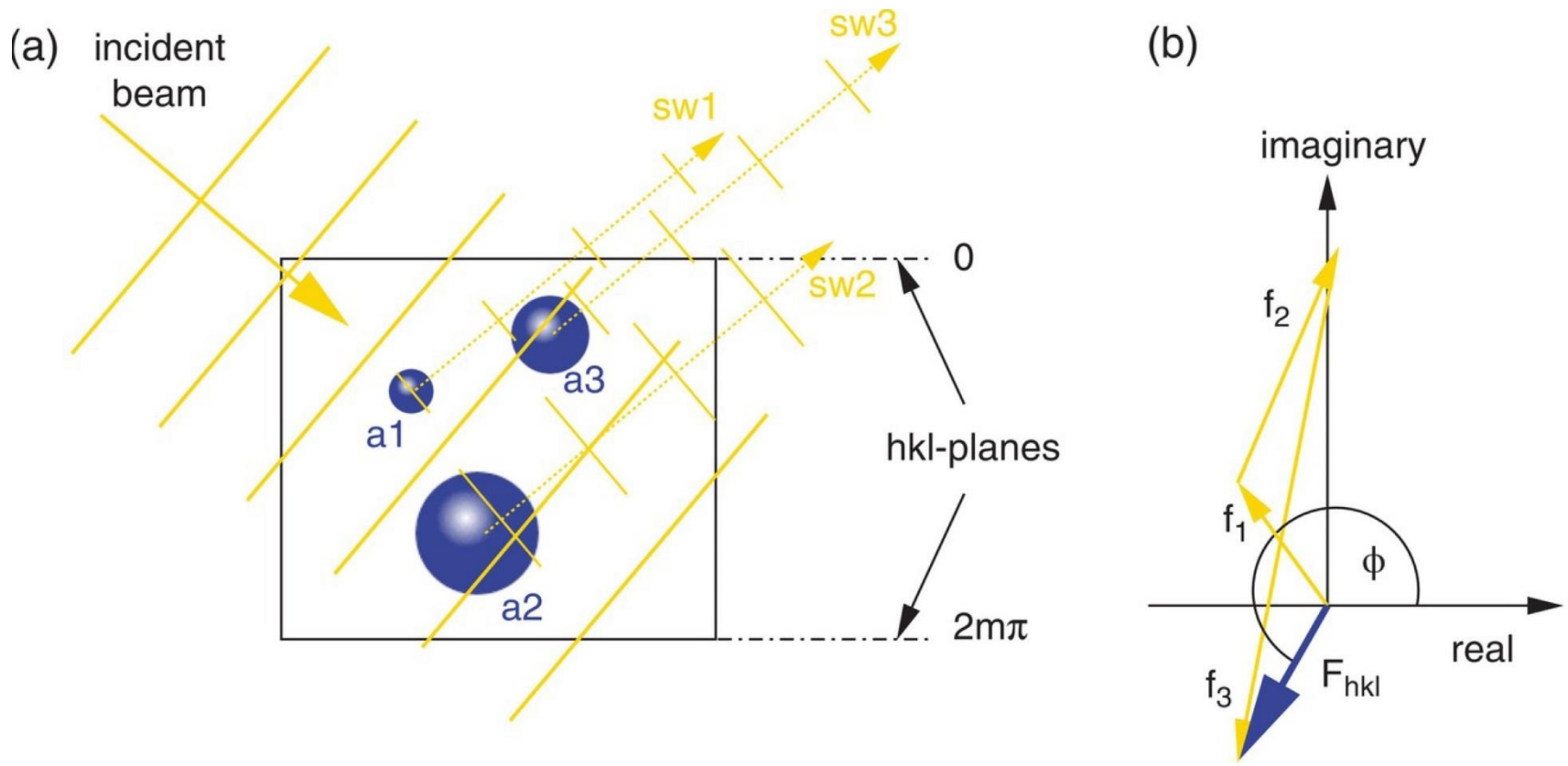

The end